

Mechanism of Hydrolysis of Phosphorylethanolamine Triesters. Multiple Catalytic Effects of an Intramolecular Amino Group

Robert A. Lazarus and Stephen J. Benkovic*

Contribution from the Department of Chemistry, The Pennsylvania State University, University Park, Pennsylvania 16802. Received December 22, 1978

Abstract: Intramolecular displacement reactions at phosphorus have been examined in a series of *N*-alkyl-*O*-(arylphenylphosphoryl)ethanolamines in 45% dioxane–water (v/v) at 35 °C. The examination of the pH–rate profiles, the detection of external buffer catalysis, and the observation of deuterium solvent effects reveal the concurrent operation of three types of P–O bond cleavage mechanisms: electrostatic catalysis by the protonated ammonium moiety of external nucleophilic attack by buffer bases at phosphorus, general-base-catalyzed intramolecular nucleophilic attack by the amino function to form the cyclic phosphoramidate, and intramolecular amine-assisted water displacement of the substituted phenol. The assignment of electrostatic rather than general acid catalysis as the role of the ammonium moiety derives from the identity in rate coefficients for nucleophilic attack by buffer species on the cationic trimethylammonium and protonated ammonium triesters. For nucleophilic fluoride attack in 85% dioxane–water this leads to a rate acceleration of ca. 10^3 relative to a triester possessing no intramolecular ammonium moiety. Structure–reactivity correlations for the electrostatic process yield values of β_{lg} dependent on the $\text{p}K_{\text{a}}$ of the nucleophile inferring a coupled transition state. A Brønsted plot for the general-base-catalyzed cyclization reaction yields a value of $\beta_{\text{gb}} \approx 0.8$ for a series of general base catalysts ($\text{p}K_{\text{a}} > 7$). Since proton removal from a putative pentacovalent intermediate would be thermodynamically favorable ($\beta_{\text{gb}} \approx 0$), the data collectively support either a concerted mechanism for the cyclization process apparently bypassing the formation of a pentacovalent intermediate with a discrete lifetime or a mechanism involving hydrogen-bonding stabilization of the rate-determining decomposition of the intermediate providing that this is faster than the diffusion away of the catalyst. In either case the lifetime of the pentacovalent intermediate is $< 10^{-12}$ s.

Introduction

The involvement of neighboring groups in phosphate ester hydrolysis may provide models for biological phosphoryl transfer reactions.¹ Neighboring group catalyses by carboxyl,² hydroxyl,³ and amide⁴ functions have been shown to involve two basic types of mechanisms: general acid catalysis of leaving-group expulsion for monoesters via the metaphosphate species, and nucleophilic attack on phosphorus involving the formation of five- or six-membered rings for di- and triesters.

The present study was initiated in order to study the effect of an amino group as a catalyst for phosphoryl transfer. Although previous investigations have implicated participation by the amine function as both a potential nucleophilic⁵ and electrophilic⁶ catalyst, our intention was to establish the relative importance of these catalytic modes and to elucidate the associated probable transition state structures. The results presented demonstrate that, in an intramolecular system, the amino function can act in at least three modes, as a nucleophile, a general base, or an electrostatic catalyst. For all modes structure–reactivity correlations derived by changing amine, buffer, and leaving-group acidities do not support stepwise mechanisms involving pentacovalent species with lifetimes $> 10^{-12}$ s despite in one case the formation of cyclic five-membered-ring products.

Experimental Section

Melting points were taken on a Fisher-Johns apparatus and are uncorrected. Microanalyses were performed by either Midwest MicroLab, Ltd., Indianapolis, Ind., or M-H-W Laboratories, Phoenix, Ariz. Infrared spectra were obtained on either a Perkin-Elmer Model 267 or 735 and were calibrated with polystyrene film. ¹H NMR spectra were recorded on a Varian Associates A-60 instrument and chemical shifts (δ) are reported relative to either tetramethylsilane or DSS. ³¹P NMR measurements were taken on a JEOL PS-100-FT spectrometer at 40.29 MHz. ³¹P NMR spectra involving an isotope shift due to ¹⁸O were recorded at 145.7 MHz on a Bruker WH360. Mass spectra (70 eV) were measured on an MS-902 AEI spectrometer and chemical ionization mass spectra were taken on a Scientific Research Instrument Corp. Biospect instrument at 1 Torr using a solids

probe and methane as the reagent gas. Ultraviolet spectra were taken on a Cary 118 instrument. Column chromatography was conducted using a 1.5 × 125 cm column packed with silica gel (Woelm, 0.032–0.063 mm) pressurized to 50 psi and eluting with chloroform. Thin layer chromatography was performed on Eastman chromogram silica sheets.

Materials. Boiled, doubly distilled, deionized water was used throughout. *p*-Dioxane was purified by the method of Fieser⁷ and stored frozen under nitrogen prior to use. All chemicals and solvents were commercially available reagent grade materials and were generally either distilled or recrystallized. Inorganic salts, acetic acid, and formic acid were analytical reagent grade and were used without further purification. Other carboxylic acids and amines employed as buffers were freshly distilled or recrystallized before use.

***p*-Nitrophenyl Phenyl Phosphorochloridate.** The procedure of Bromilow et al.^{2b} was repeated using 13.6 g (0.084 mol) of sodium *p*-nitrophenoxide and 20.2 g (0.096 mol) of phenyl phosphorodichloridate (Aldrich) in 250 mL of dry benzene at reflux for 4 h. After filtration of the sodium chloride and removal of the benzene, distillation at 170–174 °C (0.06 mmHg) afforded a yellow oil which solidified with scratching to yield 10.5 g (40%) of the desired product, mp 78 °C (lit.^{2b} 78–79 °C) from Et₂O–petroleum ether. IR (KBr): 1470 m, 1290 m, 1150 s, 930 m cm^{−1}.

***m*-Nitrophenyl Phenyl Phosphorochloridate.** A mixture of 20.0 g (0.144 mol) of *m*-nitrophenol, 30.4 g (0.144 mol) of phenyl phosphorodichloridate, and 0.3 g of dry sodium chloride was heated in an oil bath at 190 °C for 6 h. Distillation at 205 °C (0.5 mmHg) (lit.^{2b} 173–175 °C, 0.3 mmHg) afforded 24.2 g (54%) of a yellow oil which would not crystallize. IR (neat): 1595 w, 1535 s, 1480 m, 1355 s, 1310 s, 1190 s, 970 s cm^{−1}.

2-Chloro-4-nitrophenyl Phenyl Phosphorochloridate. A mixture of 4.2 g (0.024 mol) of 2-chloro-4-nitrophenol, 5.11 g (0.024 mol) of phenyl phosphorodichloridate, and 50 mg of sodium chloride was heated in an oil bath at 200 °C for 4 h. The oil solidified upon scratching to give 3.54 g (42%) of white crystals after washing with Et₂O, mp 132–133 °C. IR (KBr): 1470 m, 1190 s, 930 s cm^{−1}.

***p*-Nitrophenyl Phenyl Hydrogen Phosphate (7a).** This was prepared by the method of Dilaris and Eliopoulos⁸ to give a 56% yield of off-white crystals: mp 99 °C (benzene) (lit. 101–102, 98–100 °C^{5c}); ³¹P NMR (45% dioxane–H₂O) −11.7 ppm s.

***N*-(2-Hydroxyethyl)-2,2,2-trifluoroacetamide.** Ethyl trifluoroacetate (56.8 g, 0.4 mol) (Aldrich) in 50 mL of chloroform was added dropwise to a stirred solution of 24.4 g (0.4 mol) of ethanol-

amine (Aldrich) in 50 mL of chloroform. The solution was stirred at room temperature for 5 h, rotary evaporated to remove the solvent, and distilled at 115 °C (4.3 mmHg) to give 58.5 g (93%) of oil that crystallized upon scratching: mp 34–35 °C (lit.⁹ 36–37 °C); IR (neat) 3300 br, 1705 s, 1565 m, 1170 s, 1060 m cm^{-1} ; CIMS m/e 158 (MH^+).

2-(2,2,2-Trifluoroethylamino)ethanol. *N*-(2-Hydroxyethyl)-2,2,2-trifluoroacetamide (40 g, 0.25 mol) in 120 mL of Et_2O was added dropwise to a stirred solution of 20 g (0.526 mol) of lithium aluminum hydride in 300 mL of Et_2O at 0 °C. The mixture was then refluxed for 2 h and cooled, and excess lithium aluminum hydride was destroyed by careful addition of 20 mL of H_2O , 20 mL of 15% NaOH, and 60 mL of H_2O . The precipitated salts were filtered and the filtrate was evaporated to give an oil which was distilled at 85 °C at water aspirator pressure to afford 26 g (71%) of clear liquid: ^1H NMR (CDCl_3) δ 2.79 (t, 2, $J = 5$ Hz, CH_2N), 3.22 (q, 2, $J = 9$ Hz, CH_2CF_3), 3.64 (t, 2, $J = 5$ Hz, CH_2O); IR (CHCl_3) 3600 w, 3320 br, 1650 m, 1250 s, 1150 s, 1050 cm^{-1} ; CIMS m/e 144 (MH^+).

***N*-Ethyl-*N*-(*o*-nitrophenylsulfenyl)ethanolamine.** To a cold, stirred solution of 3.51 g (0.0394 mol) of 2-(ethylamino)ethanol (Aldrich) in 50 mL of CH_2Cl_2 was added 3.75 g (0.0197 mol) of *o*-nitrophenylsulfenyl chloride (Aldrich) in 50 mL of CH_2Cl_2 over 20 min. The solution was stirred for 2 h at room temperature, then washed with H_2O , 1 N HCl, and H_2O to neutrality. The organic layer was dried over anhydrous MgSO_4 , filtered, and rotary evaporated to give 4.88 g of an orange oil, which crystallized upon standing. Recrystallization from benzene–hexane gave 4.0 g of orange needles (84%): mp 45–46 °C; MS m/e 242 (M^+), 211; 154; R_f (CHCl_3) 0.36.

***N*-(*o*-Nitrophenylsulfenyl)-*N*-(2,2,2-trifluoroethyl)ethanolamine.** This was prepared as above in 70% yield: mp 66–67 °C (benzene–hexane); ^1H NMR (CDCl_3) δ 2.20 (s, 1, OH), 3.35 (t, 2, $J = 5$ Hz, CH_2N), 3.75 (q, 2, $J = 9$ Hz, CH_2CF_3), 3.83 (t, 2, $J = 5$ Hz, CH_2O), 7.0–8.3 (m, 4, aromatic H); MS m/e 296 (M^+); R_f (CHCl_3) 0.37.

Dissymmetric Alkyl Diaryl Phosphotriesters. These were prepared from the dissymmetric diaryl phosphorochloridate and the alcohol in dry pyridine (freshly distilled from BaO, then CaH_2). A typical procedure was to slowly add 5 mmol of the dissymmetric phosphorochloridate to an ice bath cooled, stirred solution of 5 mmol of the alcohol in 10 mL of dry pyridine. After a few minutes, pyridinium hydrochloride would usually precipitate out of the solution. Stirring was continued at room temperature overnight. The mixture was taken up in 20 mL of Et_2O and 20 mL of H_2O . The aqueous layer was separated and extracted three times with 10 mL of Et_2O and the combined organic extracts were washed with 2 N HCl and H_2O to neutrality, dried (MgSO_4), and concentrated to an oil. If TLC of the oil showed a mixture of compounds, then the oil was chromatographed on silica using CHCl_3 as the eluent.

Ethyl *p*-Nitrophenyl Phenyl Phosphate (10): white needles (84%); mp 46–47 °C (ether–pentane); ^1H NMR (CCl_4) δ 1.40 (t, 3, $J = 7$ Hz, CH_3), 4.37 (m, 2, CH_2), 7.35 (m, 7, aromatic H), 8.31 (d, 2, H ortho to NO_2); ^{31}P NMR (CDCl_3) δ -13.1 s; UV (H_2O) λ_{max} 272 nm (ϵ 9415).

***N*-Ethyl-*N*-(*o*-nitrophenylsulfenyl)-*O*-(*p*-nitrophenylphenylphosphoryl)ethanolamine:** orange oil (85%).

***N*-Ethyl-*N*-(*o*-nitrophenylsulfenyl)-*O*-(*m*-nitrophenylphenylphosphoryl)ethanolamine:** orange oil (90%); IR (neat) 1520 s, 1370 s, 1300 s, 970 cm^{-1} ; R_f (CH_3CN) 0.62.

***N*-Ethyl-*N*-(*o*-nitrophenylsulfenyl)-*O*-(2-chloro-4-nitrophenylphenylphosphoryl)ethanolamine:** orange oil (88%); IR (CHCl_3) 1600 w, 1520 s, 1350 s, 1310 w, 1210 s, 1040 w cm^{-1} ; R_f (CHCl_3) 0.66.

***N*-(*o*-Nitrophenylsulfenyl)-*N*-(2,2,2-trifluoroethyl)-*O*-(*p*-nitrophenylphenylphosphoryl)ethanolamine:** orange oil (95%); ^1H NMR (CDCl_3) δ 3.3–3.9 (m, 4, CH_2NCH_2), 4.42 (m, 2, CH_2O), 7.0–7.6 (m, 11, aromatic H), 8.0 (d, 2, H ortho to NO_2); IR (CHCl_3) 1590 m, 1520 m, 1490 m, 1340 s, 1300 s, 1160 s, 950 cm^{-1} .

***N*-Alkyl-*O*-(arylphenylphosphoryl)ethanolamine Hydrochloride.** These compounds were prepared by bubbling anhydrous HCl through an ether solution of the corresponding *N*-protected *o*-nitrophenylsulfenyl compound. An oil precipitated out after several minutes and usually crystallized upon standing overnight. The oil was sometimes triturated with anhydrous HCl– Et_2O to induce crystallization. The compounds could be recrystallized from acetonitrile–ether. Yields ranged from 60 to 90%.

***N*-Ethyl-*O*-(*p*-nitrophenylphenylphosphoryl)ethanolamine Hydrochloride (1a):** mp 102–103 °C; ^1H NMR ($\text{Me}_2\text{SO}-d_6$) δ 1.17 (t, 3, $J = 7$ Hz, CH_3), 2.7–3.4 (m, 4, CH_2NCH_2), 4.67 (m, 2, CH_2O),

7.37 (m, 7, aromatic H), 8.33 (d, 2, H ortho to NO_2); ^{31}P NMR (45% dioxane– H_2O) δ -13.3 s; free amine δ -12.7 s; IR (KBr) 2750 br, 2460 m, 1590 s, 1525 s, 1490 s, 1345 s, 1300 s, 1190 s, 1080 m, 1020 s, 955 cm^{-1} ; UV (45% dioxane– H_2O) λ_{max} 268 nm (ϵ 9200).

Anal. Calcd for $\text{C}_{16}\text{H}_{20}\text{N}_2\text{O}_6\text{P}\text{Cl}$: C, 47.73; H, 5.01; N, 6.96. Found: C, 47.37; H, 5.14; N, 6.70.

***N*-Ethyl-*O*-(*m*-nitrophenylphenylphosphoryl)ethanolamine Hydrochloride (1b):** mp 77 °C; ^1H NMR ($\text{Me}_2\text{SO}-d_6$) δ 1.28 (t, 3, $J = 7$ Hz, CH_3), 2.8–3.4 (m, 4, CH_2NCH_2), 4.73 (m, 2, CH_2O), 7.51 (s, 5, Ph), 7.99–8.25 (m, 4, aromatic H); ^{31}P NMR (45% dioxane– H_2O) δ -12.8 s; free amine δ -12.2 s; IR (KBr) 2740 br, 2460 br, 1590 w, 1530 s, 1350 m, 1300 s, 1195 s, 970 cm^{-1} ; UV (45% dioxane– H_2O) λ_{max} 261 nm.

Anal. Calcd for $\text{C}_{16}\text{H}_{20}\text{N}_2\text{O}_6\text{P}\text{Cl}$: C, 47.73; H, 5.01; N, 6.96. Found: C, 47.61; H, 4.76; N, 6.91.

***N*-Ethyl-*O*-(2-chloro-4-nitrophenylphenylphosphoryl)ethanolamine Hydrochloride (1c):** mp 101–102 °C; ^{31}P NMR (45% dioxane– H_2O) δ -13.8 s; free amine δ -13.2 s; IR (KBr) 2780 br, 2460 w, 1590 w, 1530 m, 1480 s, 1350 s, 1200 s, 960 cm^{-1} ; UV (45% dioxane– H_2O) λ_{max} 266 nm.

Anal. Calcd for $\text{C}_{16}\text{H}_{19}\text{N}_2\text{O}_6\text{P}\text{Cl}_2$: C, 43.95; H, 4.38; N, 6.41. Found: C, 44.10; H, 4.59; N, 6.50.

***N*-(2,2,2-Trifluoroethyl)-*O*-(*p*-nitrophenylphenylphosphoryl)ethanolamine Hydrochloride (3a):** mp 82–84 °C; ^1H NMR ($\text{Me}_2\text{SO}-d_6$) δ 3.33 (t, 2, $J = 5$ Hz, CH_2N), 3.92 (q, 2, $J = 9.5$ Hz, CH_2CF_3), 4.63 (q, 2, $J = 5$ Hz, CH_2O), 7.21 (m, 7, aromatic H), 8.25 (d, 2, H ortho to NO_2); ^{31}P NMR (45% dioxane– H_2O) free amine δ -12.8 s; IR (KBr) 2700–2300 br, 1585 m, 1510 m, 1475 m, 1340 s, 1160 s cm^{-1} .

Anal. Calcd for $\text{C}_{16}\text{H}_{17}\text{N}_2\text{O}_6\text{PClF}_3$: C, 42.07; H, 3.75; N, 6.13. Found: C, 41.72; H, 3.94; N, 5.99.

***N,N*-Dimethyl-*O*-(*p*-nitrophenylphenylphosphoryl)ethanolamine Hydrochloride (2a).** To a solution of 0.73 g (0.0082 mol) of freshly distilled *N,N*-dimethylethanolamine (Aldrich) in 10 mL of dry pyridine at 5 °C was added 2.57 g (0.0082 mol) of *p*-nitrophenyl phenyl phosphorochloridate. After 5 min the solution solidified and was diluted with 50 mL of Et_2O and stirred overnight. The white crystals were filtered and recrystallized from acetonitrile–ether several times to give 3.0 g of white crystals (91%); mp 127–128 °C; ^1H NMR ($\text{Me}_2\text{SO}-d_6$) δ 2.79 (s, 6, CH_3), 3.5 (m, 2, CH_2N), 4.7 (m, 2, CH_2O), 7.3 (m, 7, aromatic H), 8.3 (d, 2, H ortho to NO_2); ^{31}P NMR (45% dioxane– H_2O) free amine δ -12.9 s; IR (KBr) 2750–2300 br, 1590 w, 1520 s, 1480 s, 1340 s, 1290 m, 1190 m, 940 w cm^{-1} ; UV (45% dioxane– H_2O) λ_{max} 270 nm.

Anal. Calcd for $\text{C}_{16}\text{H}_{20}\text{N}_2\text{O}_6\text{P}\text{Cl}$: C, 47.73; H, 5.01; N, 6.96. Found: C, 47.93; H, 5.53; N, 7.04.

***N,N*-Dimethyl-*O*-(*m*-nitrophenylphenylphosphoryl)ethanolamine Hydrochloride (2b).** This was prepared as above to give white crystals from acetonitrile–ether in 86% yield: mp 93–94 °C; ^1H NMR ($\text{Me}_2\text{SO}-d_6$) δ 2.78 (s, 6, CH_3), 3.50 (m, 2, CH_2N), 4.75 (m, 2, CH_2O), 7.32 (s, 5, Ph), 7.95 (m, 4, aromatic H); IR (KBr) 2700–2300 br, 1590 w, 1530 s, 1350 s, 1300 s, 970 cm^{-1} .

Anal. Calcd for $\text{C}_{16}\text{H}_{20}\text{N}_2\text{O}_6\text{P}\text{Cl}$: C, 47.73; H, 5.01; N, 6.96. Found: C, 47.15; H, 5.32; N, 7.08.

***O*-(*p*-Nitrophenylphenylphosphoryl)choline Iodide (4a).** The above procedure was repeated using 0.231 g (0.001 mol) of choline iodide, 1.5 mL of dry pyridine, 0.314 g (0.001 mol) of *p*-nitrophenyl phenyl phosphorochloridate, and 5 mL of Et_2O . Recrystallization from acetonitrile–ether afforded 0.21 g of pale yellow crystals (42%); mp 127–129 °C; ^1H NMR (CH_3CN) δ 3.15 (s, 9, CH_3), 3.9 (m, 2, CH_2N), 4.8 (m, 2, CH_2O), 7.33 (s, 7, aromatic H), 8.30 (d, 2, H ortho to NO_2); ^{31}P NMR (45% dioxane– H_2O) δ -13.5 s; IR (KBr) 1590 w, 1520 m, 1485 s, 1355 s, 1300 s, 1230 w, 1180 m, 960 s, 940 cm^{-1} .

Anal. Calcd for $\text{C}_{17}\text{H}_{22}\text{N}_2\text{O}_6\text{PI}$: C, 40.18; H, 4.36; N, 5.51; I, 24.97. Found: C, 39.68; H, 4.42; N, 5.20; I, 24.75.

3-Ethyl-2-oxo-2-phenoxy-1,3,2-oxazaphospholidine (6, $\text{R}_1 = \text{Et}$). This was prepared by the method of Brown et al.¹⁰ The oil distilled at 145–147 °C (0.15 mmHg) to give a 47% yield of clear, colorless product: ^1H NMR (CDCl_3) δ 1.22 (t, 3, $J = 7.5$ Hz, CH_3), 3.03 (q, 2, $J = 7.5$ Hz, CH_2CH_3), 3.25 (m, 2, CH_2N), 4.12 (m, 2, CH_2O), 7.22 (s, 5, Ph); ^{31}P NMR (45% dioxane– H_2O) δ +17.4 s; IR (CCl_4) 2980 m, 2870 m, 1595 s, 1485 s, 1390 m, 1275 s, 1190 s, 1020 s, 925 cm^{-1} ; MS m/e 227 (M^+), 134 ($\text{M} - \text{OPh}$); UV (H_2O) λ_{max} 260 nm.

Anal. Calcd for $\text{C}_{10}\text{H}_{14}\text{NO}_3\text{P}$: C, 52.86; H, 6.21; N, 6.17. Found: C, 52.77; H, 6.15; N, 5.93.

***N*-Ethyl-*O*-phenylphosphorylethanolamine (5, $\text{R}_1 = \text{Et}$; $\text{R}_2 = \text{H}$).**

This was prepared by hydrolysis of the cyclic phosphoramidate (**6**, $R_1 = \text{Et}$) in aqueous acidic acetonitrile. The solvents were lyophilized off and the resulting white crystals were recrystallized from MeOH-Et₂O to give pure white product in 60% yield: mp 197–199 °C; ¹H NMR (D₂O) δ 1.29 (t, 3, $J = 8$ Hz, CH₃), 3.17 (q, 2, $J = 8$ Hz, CH₂CH₃), 3.33 (t, 2, $J = 6$ Hz, CH₂N), 4.28 (t, 2, $J = 6$ Hz, CH₂O), 7.43 (s, 5, Ph); ³¹P NMR (45% dioxane-H₂O) δ -5.2 s; free amine -4.8 s; IR (KBr) 2980 s, 2720 s, 2490 s, 1590 w, 1490 w, 1220 s, 1075 s, 1030 s, 890 s, 760 s cm⁻¹; UV (H₂O) λ_{max} 262 nm.

Anal. Calcd for C₁₀H₁₆NO₄P: C, 48.98; H, 6.58; N, 5.71. Found: C, 48.76; H, 6.52; N, 5.50.

The hydrolysis of **6** ($R_1 = \text{Et}$) was also carried out in H₂¹⁸O to yield **5** ($R_1 = \text{Et}$; $R_2 = \text{H}$) containing one ¹⁸O bound to the phosphorus. The physical data were identical with those of the ¹⁶O isomer except for the ³¹P NMR. The isotopic shift of the ¹⁸O on the phosphorus caused an upfield shift of 4.2 Hz in water at 145.7 MHz relative to the ¹⁶O isomer.¹¹

Potassium acetate (76 atom % ¹⁸O enrichment) was prepared by heating 0.157 g (0.0026 mol) of glacial acetic acid in 0.30 mL (0.015 mol) of H₂¹⁸O (99.3 atom % enrichment, Isotope Labeling Corp., Whippany, N.J.) at 85 °C for 42 h, followed by adjustment of the pH to 7.3 with KOH and lyophilization. The hygroscopic crystals were dried at 110 °C.

Analysis of the ¹⁸O content was performed by converting a sample of the anhydrous potassium acetate to methyl acetate with methyl trifluoromethylsulfonate (Aldrich). The vapor was injected into a Finnigan GC-MS 3200 instrument employing a 5 ft \times 2 mm column of Poropak N, 80–100 mesh at 175 °C. Integration of the *m/e* 74, 76, and 78 peaks gave values of 6.1, 34.4, and 59.5%, respectively, or an overall enrichment of 76 atom % ¹⁸O.

Dissociation Constants and pH Measurements. pK_a determinations were performed on a Radiometer TTTlc autotitrator at an ionic strength of 0.2 (KCl) at 35 °C in a 45% (v/v) dioxane-H₂O medium.¹² pH measurements were taken with a Radiometer GK2302C glass electrode at 35 °C and were corrected for medium effects using the equation $\text{pH} = B + \log U_H$ where B is the actual pH meter reading and $\log U_H = -0.06$ as determined in this medium by the method of Irving and Mahnot.¹³ The pK_a s of the buffers were determined either by half-neutralization or potentiometric titration. The dissociation constant of water at 35 °C in 45% dioxane-water (v/v) is 3.63×10^{-16} M.¹⁴ The K_w of D₂O was calculated to be 5.83×10^{-17} M² by assuming that the change in $K_w(\text{D}_2\text{O})$ from 25 to 35 °C is proportional to the change in $K_w(\text{H}_2\text{O})$ from 25 to 35 °C. Measurements in 45% dioxane-D₂O were calculated from the equation $\text{pD} = \text{pH meter reading} + 0.29$.¹⁵ The dissociation constants change in going from H₂O to D₂O by the empirical equation $pK_a(\text{D}_2\text{O}) = 1.02 pK_a(\text{H}_2\text{O}) + 0.41$.¹⁶ The pK_a s of the amino groups of the phosphotriesters and the buffer species were corrected by this equation with the assumption that the same effect holds in a 45% dioxane-aqueous medium. pH measurements in aqueous media were performed at 35 °C in the usual manner; pK_a measurements were again determined by half-neutralization.

Apparatus. A Gilford Model 2000, 220, or 240 spectrophotometer equipped with a thermostated cuvette holder (± 0.1 °C) was used for kinetic measurements. All pH determinations were made with a Radiometer Model 22 pH meter equipped with a Model PHA 630 Pa scale expander and a Radiometer GK2302C electrode.

Kinetics. All kinetic experiments were performed in 45% (v/v) dioxane-water at 35.0 ± 0.1 °C, $\mu = 0.2$ (KCl), unless stated otherwise. Stock solutions ($\sim 10^{-3}$ M) of the phosphates were prepared in acetonitrile which has been purified by distillation from P₂O₅ and CaH₂. The stock was stored at 5 °C between experiments with no decomposition detected. Reactions were initiated by the addition of 0.02–0.05 mL of the stock solution to 2 mL of a buffer solution in a cuvette which had been equilibrated for 15 min in the cell holder. The hydrolysis of phosphates **1–4** and **10** was monitored for nitrophenol release at either 406 (*p*-NO₂), 404 (*m*-NO₂), or 408 nm (2-Cl-4-NO₂) in basic medium. The reactions were followed at 320 nm as the nitrophenols became protonated. The hydrolysis of the cyclic phosphoramidate (**6**, $R_1 = \text{Et}$) was followed at 263 nm ($\sim 10^{-3}$ M) in acidic buffers for the ring-opening reaction and at 287 nm ($\sim 4 \times 10^{-4}$ M) in basic media for the release of phenolate anion. The extinction coefficients at 263 nm are 328 and 556 for compounds **6** ($R_1 = \text{Et}$) and **5** ($R_1 = \text{Et}$; $R_2 = \text{H}$), respectively. Reactions were generally followed for at least 3 half-lives and infinity readings taken after 10, except for very slow reactions, which were followed by the method of initial rates. The pH

of the medium was measured at 35 °C before and after each kinetic run; those runs exhibiting pH drift of greater than ± 0.03 were discarded.

The observed pseudo-first-order rate constants for the hydrolysis of **1–4**, **6** ($R_1 = \text{Et}$), and **10** were calculated from the slopes of linear plots of $\ln(\text{OD}_\infty - \text{OD}_t)$ against time. Plots were generally linear to 3 half-lives. Duplicate runs agreed with $\pm 3\%$. The values of k_{obsd} obtained for **1–3** were found to be composed of two parallel first-order reactions, one (k^{PO}) being the release of the nitrophenol due to P–O bond cleavage and the other (k^{CO}) being the release of the nitrophenyl phenyl phosphate (**7**) due to C–O bond cleavage. Since both pathways for the disappearance of the triesters are first order, the fraction of the reaction proceeding via P–O bond cleavage can be obtained by determining the amount of the nitrophenol formed (OD_{np}) and dividing by the total amount possible.¹⁷ The rate constant for nitrophenol release is equal to the fraction of P–O bond cleavage times the total rate; k^{CO} can then be determined by subtracting k^{PO} from k_{obsd} . OD_{np} was determined by adding a 1-mL aliquot of the final solution to 1 mL of 0.36 M KOH in 45% dioxane-water and reading OD₄₀₆, OD₄₀₄, or OD₄₀₈ for *p*-nitrophenol (ϵ_{406} 20 970), *m*-nitrophenol (ϵ_{404} 1495), or 2-chloro-4-nitrophenol (ϵ_{408} 18 700). Extinction coefficients were all determined from the pure nitrophenol in 45% dioxane-water at 35 °C. Since no other species absorb at 406 nm and *p*-nitrophenyl phenyl phosphate was shown to hydrolyze very slowly when subjected to identical conditions,¹⁸ $\text{OD}_{\text{np}} = 2\text{OD}_{406}$. $(\text{OD}_{\text{np}})_{\text{total}}$ was determined from the extinction coefficient of the nitrophenol and the initial concentration of the triester.

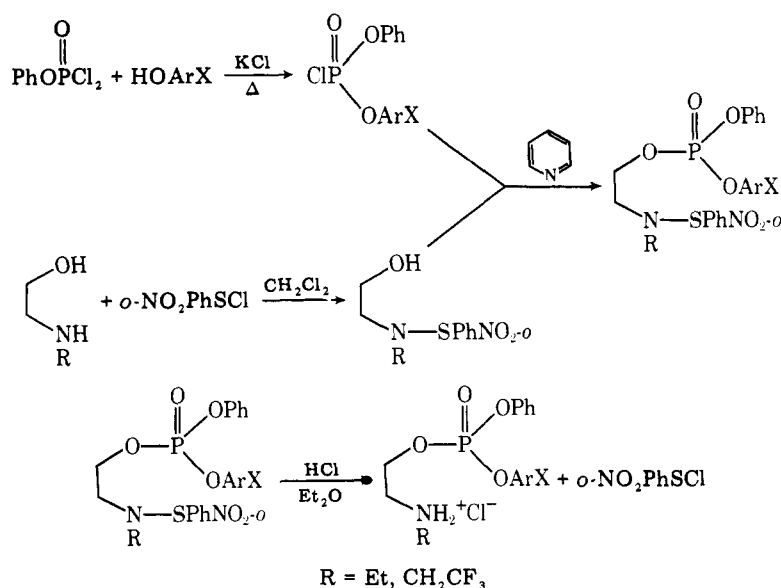
The concentration of buffer species was generally 0.05–0.15 M. From three to six serially diluted buffer solutions were employed at each pH. The pH of the serial dilutions agreed within 0.03 pH unit. The spontaneous hydrolysis for k^{PO} was obtained as the intercept of a plot of k^{PO} vs. buffer concentration. k^{CO} was independent of buffer concentration. Second-order buffer-catalyzed rates were determined from the slopes of k^{PO} vs. buffer concentration. Catalysis by fluoride was studied using both 0.05 M imidazole and 0.05 M acetate as buffers at a pH where fluoride exists primarily as F⁻. Catalysis by acetate or imidazole was negligible compared with fluoride catalysis. Experiments to detect an acyl phosphate intermediate were performed in a 0.5 M acetate, 0.075 M hydroxylamine, 45% dioxane-water media at pH 5.2 and monitored by the method of Bruce and Bruno.¹⁹ Repetitive scans for the hydrolysis in acetate buffers were performed by a Cary 118 instrument. The solvent isotope effect of **2a** and **4a** was determined using 45% dioxane-D₂O (99.7%, Merck Sharpe and Dohme) at pD 10.55.

Product Analysis. The hydrolysis products were primarily investigated using ³¹P NMR spectroscopy. The various phosphates were hydrolyzed under identical conditions with those employed for determining their rates. Between 30 and 70 mg of compound was placed in a 10-mm NMR tube and 2 mL of buffer solution at 35 °C added. Buffers employed were acetate, imidazole, 2-methylimidazole, Tris, triethylamine, cacodylate, ethanolamine, and fluoride. Buffer concentrations were all 0.5 M in 45% dioxane-water except fluoride, which was 0.05 M in either 0.24 M imidazole or 0.2 M acetate. The pH of the solution was measured before and after the hydrolysis and the amount of buffer in its free base (or acid) form calculated from its pK_a . The spectrum was recorded by a JEOL PS-100 FT spectrometer at a frequency of 40.29 MHz using 45° pulse and a repetition rate of 2.2 s. Spectra could be obtained within 20 s in this manner. Scans were made ± 25 ppm of 85% H₃PO₄. A capillary tube filled with D₂O was inserted and used as the heteronuclear lock. Chemical shifts are referenced to an external standard of 85% H₃PO₄ with a 5-mm tube of D₂O as the lock; upfield shifts (to the right) are reported as being negative, in accordance with the new convention.²⁰ For those experiments where the integration of the peaks is directly proportional to the amount of compound, the sample was pulsed at 45° using a pulse rate of 30 s. This ensured that the nuclei were relaxed before each pulse so that the peaks were not saturated.

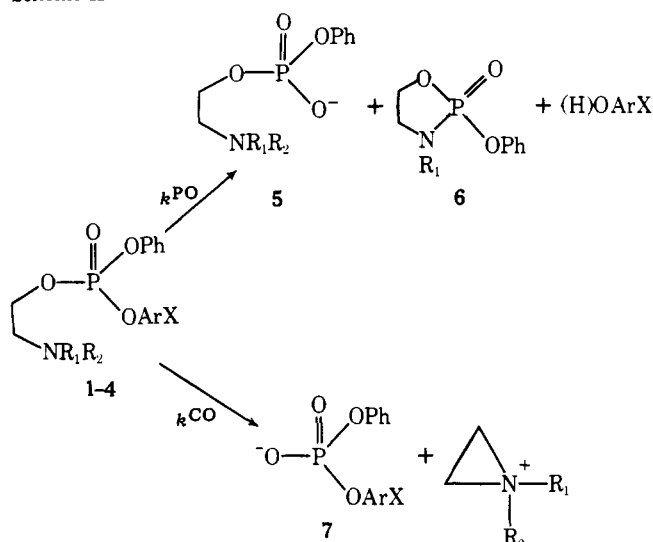
³¹P NMR experiments involving **1a** and **4a** with ¹⁸O-acetate and H₂¹⁸O were run under identical conditions as above on a Bruker WH360. The phosphate concentration was 10–30 mM and acetate was ca. 0.4 M (80% free base form) so that the acetate-catalyzed pathway carried at least 70% of the reaction flux.

¹⁹F NMR experiments were performed on a JEOL PS-100 FT spectrometer at a frequency of 93.65 MHz, repetition rate of 2 s, and spectrum width of 10 kHz. Values are reported as ϕ^* where $\phi^* = \phi_R^* + \delta_S$.²¹ Spectra were taken of solutions in a 5-mm NMR tube after

Scheme I



Scheme II



	R_1	R_2	X		R_1	R_2	X
1a	Et	H	<i>p</i> -NO ₂	2b	Me	Me	<i>m</i> -NO ₂
1b	Et	H	<i>m</i> -NO ₂	3a	CF ₃ CH ₂	H	<i>p</i> -NO ₂
1c	Et	H	2-Cl-4-NO ₂				
2a	Me	Me	<i>o</i> -NO ₂	4a	NMe ₃ ⁺	I ⁻	<i>p</i> -NO ₂

128 scans. Samples were 0.05 M in phosphate triester, 0.05 M fluoride, 0.05 M acetate, and 45% dioxane-water containing 15% D₂O as the heteronuclear lock.

¹H NMR experiments to determine possible amide formation were performed on a Varian A-60 instrument. Hydrolyses were carried out in 5-mm NMR tubes containing 30 mg of compound in a solution of 0.5 M acetate (80% free base form) in 50% Me₂SO-*d*₆-D₂O.

Results

Synthesis. A general procedure for the synthesis of the required dissymmetric β-aminophosphotriesters is displayed in Scheme I. The success of this synthesis stems from the use of the *o*-nitrophenylsulfenyl chloride²² to block the amino function permitting unequivocal formation of the O-phosphorylated ethanolamine followed by its facile removal under mild acidic conditions to form the stable ammonium salt. For the synthesis of the Me₂N- and Me₃N⁺-substituted phosphotriesters, protection of the amino function is not necessary, with the desired triester formed directly from the respective dissymmetric

phosphorochloridate and N-substituted ethanolamine in dry pyridine.

Lyate Species Catalysis. The hydrolyses of the phosphate triesters 1–4 were investigated over the pH range 2–11 in 45% (v/v) dioxane–water at 35 °C ($\mu = 0.2$, KCl). A general scheme for their hydrolysis is given in Scheme II. The observed pseudo-first-order rate constant k_{obsd} is the sum of rate constants for both P–O and C–O bond cleavage processes with the rate constant for the P–O reaction (k^{PO}) determined by measuring the fraction of (H)OArX produced. All of the triesters except 4a have competing pathways with their proportions dependent upon pH, buffer concentration, and the nature of both the leaving group and the amino function. The data for the hydrolysis reactions involving P–O bond cleavage are consistent with the following rate laws:

$$k^{\text{PO}} = (k_{\text{H}}a_{\text{H}} + k_{\text{H}_2\text{O}} + k_{\text{OH}}a_{\text{OH}}) \left(\frac{K_{\text{a}}}{K_{\text{a}} + a_{\text{H}}} \right) \quad (1)$$

$$k^{\text{PO}} = k^{\text{PO}} + k_{\text{N}}[\text{B}]_{\text{T}} \left(\frac{K_{\text{a}}^{\text{B}}}{K_{\text{a}}^{\text{B}} + a_{\text{H}}} \right) \left(\frac{a_{\text{H}}}{K_{\text{a}} + a_{\text{H}}} \right) + k_{\text{B}}[\text{B}]_{\text{T}} \left(\frac{K_{\text{a}}^{\text{B}}}{K_{\text{a}}^{\text{B}} + a_{\text{H}}} \right) \left(\frac{K_{\text{a}}}{K_{\text{a}} + a_{\text{H}}} \right) \quad (2)$$

where k_{H} , $k_{\text{H}_2\text{O}}$, and k_{OH} are the rate coefficients associated with lyate species hydrolysis, K_{a}^{B} is the dissociation constant for the buffer species, and K_{a} is the dissociation constant for the amino group in 1–3. The dependence on pH of k^{PO} for 1a is shown in Figure 1. Values of k^{PO} were obtained from the ordinal intercepts of plots of k^{PO} against total buffer concentration (Figures 2 and 3). All rate constants defined in eq 1 have been determined using a multiple regression analysis²³ and are given in Table I. In the case of 2 the term $k_{\text{OH}} = 0$; for 1b and 2b (*m*-nitrophenol as the leaving group) the term k_{H} was too small to be accurately measured. For 4a, only the rate coefficients $k_{\text{H}_2\text{O}}$ and k_{OH} were determined.

The dependence on pH of the competing C–O bond cleavage process is similar for 1–3 and is illustrated for 2a in Figure 4. Data for the pH–rate profile is described by the equation

$$k^{\text{CO}} = k_{\text{H}_2\text{O}}^{\text{CO}} \left(\frac{K_{\text{a}}}{K_{\text{a}} + a_{\text{H}}} \right) \quad (3)$$

where $k_{\text{H}_2\text{O}}^{\text{CO}}$ is the rate coefficient for amine-assisted C–O bond cleavage. No buffer catalysis was observed. Values for $k_{\text{H}_2\text{O}}^{\text{CO}}$ also are listed in Table I. The fraction of C–O bond

Table I. Dissociation^a and Rate^b Constants for the Hydrolysis of Phosphate Triesters 1-4 (45% Dioxane-H₂O, *T* = 35 °C, μ = 0.2 (KCl))

compd	p <i>K</i> _a amine	p <i>K</i> _a XArOH	<i>k</i> _H , M ⁻¹ min ⁻¹	<i>k</i> _{H₂O} , min ⁻¹	<i>k</i> _{OH} , M ⁻¹ min ⁻¹	<i>k</i> _{H₂O} ^{CO} , min ⁻¹
1a	7.64	7.73	3000	0.015 8	6.13 × 10 ⁴	0.055
1b	7.64	9.10		0.008 0	1.03 × 10 ⁴	0.041
1c	7.64	6.01	8.0 × 10 ⁴	0.358	6.25 × 10 ⁵	0.135
2a	6.87	7.73	500	0.021 0		0.067
2b	6.87	9.10		0.011 3		0.063
3a	2.54	7.73	0.026	0.000 15	1200	0.0022
4a		7.73		0.000 05	1600	

^a Determined by potentiometric titration.¹² Values reported are accurate to ±0.05 p*K*_a unit. ^b Determined by multiple regression analysis.²³

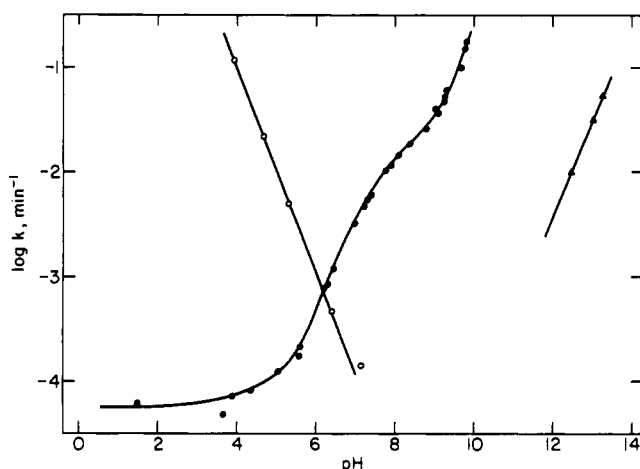


Figure 1. Dependence on pH of the observed pseudo-first-order rate constants for P-O bond cleavage for the hydrolysis of **1a** (●, *k*_{O^{PO}}) extrapolated to zero buffer concentration at 35 °C, 45% dioxane-water (v/v), μ = 0.2 (KCl). The solid line is calculated from eq 1 and the rate constants in Table I. The pH-rate profile for the hydrolysis of the cyclic phosphoramidate **6** (*R*₁ = Et) under identical conditions is shown for both P-N bond cleavage (○, *k*_{H^{PN}}) and exocyclic P-O bond cleavage (▲, *k*_{OH^{PO}}) pathways. The solid lines are calculated from eq 4 and the values reported in the text.

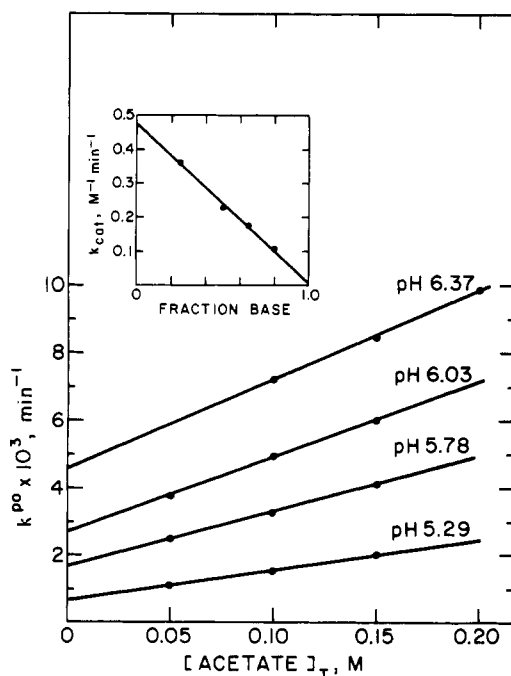


Figure 2. Dependence of the observed pseudo-first-order rate constants for P-O bond cleavage for the hydrolysis of **2a** on the concentration of acetate buffers at four buffer ratios at 35 °C, 45% dioxane-water (v/v), μ = 0.2 (KCl). The inset shows a plot of *k*_{cat} [= (*k*^{PO} - *k*_{O^{PO}})/([B]_T(*K*_a/(*K*_a + *a*_H)))] vs. the fraction free base form of acetate.

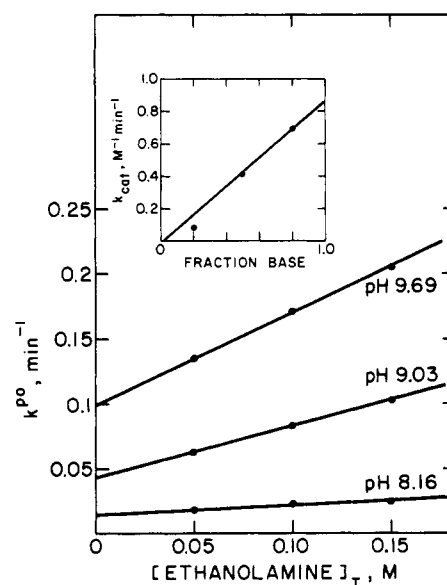


Figure 3. Dependence of the observed pseudo-first-order rate constants for P-O bond cleavage for the hydrolysis of **1a** on the concentration of ethanolamine buffers at three buffer ratios at 35 °C, 45% dioxane-water (v/v), μ = 0.2 (KCl). The inset shows a plot of *k*_{cat} [= (*k*^{PO} - *k*_{O^{PO}})/([B]_T(*K*_a/(*K*_a + *a*_H)))] vs. the fraction free base form of ethanolamine.

cleavage is maximal (0.73, 0.85, and 0.19 for **1a-c**, respectively) at neutral pH (6-8) and approaches zero in both acidic and basic media.

The pH-rate profile for the hydrolysis of the cyclic phosphoramidate **6**, where *R*₁ = Et, is included in Figure 1 and is described by the rate law

$$k_{\text{obsd}} = k_{\text{H}^{\text{PN}}}a_{\text{H}} + k_{\text{OH}^{\text{PO}}}a_{\text{OH}} \quad (4)$$

At pH < 7, hydrolysis is hydronium ion catalyzed with *k*_{H^{PN}} = 973 M⁻¹ min⁻¹ and proceeds via P-N bond fission to yield **5** (*R*₁ = Et; *R*₂ = H); at pH > 12 hydrolysis results from attack by hydroxide with *k*_{OH^{PO}} = 1.92 M⁻¹ min⁻¹ and proceeds via expulsion of phenoxide to give the monoanionic cyclic phosphoramidate **8**. No buffer catalysis was detected. Hudson et al.¹⁰ have studied the alkaline hydrolysis (0.01-0.05 M OH⁻) of **6** (*R*₁ = Me) and have reported a 91% formation of phenoxide with the remaining products equally divided between fission of the cyclic P-N and P-O bonds. In the presence of 0.028 M OH⁻ and 45% (v/v) dioxane-H₂O at 35 °C, the observed rates of hydrolysis for phenoxide expulsion of **1a-c** and **6** (*R*₁ = Et) are identical (0.051 ± 0.002 min⁻¹).

Buffer Catalysis. Table II summarizes the second-order rate constants, expressed as *k*_N, for nucleophilic attack by the free form of the buffer on the conjugate acid forms of the triesters **1-3**. Values of the slopes of plots of *k*^{PO} corrected for the mole fraction amine in the free base form (Figures 2 and 3) were

Table II. Experimental Conditions and Rate Constants^a for Nucleophilic Buffer Catalysis (k_N , $M^{-1} \text{ min}^{-1}$) of Phosphate Triester Hydrolysis^b

buffer	$pK_a^{B,c}$	concn ^d range, M	mole fraction ^e free base form	1a	2a	3a ^f	4a	1b	2b	1c
H ₂ O ^g	-1.49 ^h	30.8		2.23×10^{-6}	2.19×10^{-6}	2.40×10^{-6} ^a 4.87×10^{-6}	1.62×10^{-6}			5.95×10^{-5}
cyanoacetate (CNAc)	3.40	0.05-0.15	0.50-0.75	0.0010	0.00138					0.038
pyridine (PYR)	4.35	0.05-0.15	0.80		0.0052				0.0020	
formate (HCOO ⁻)	4.47	0.08-0.16	0.50	0.0076						
methoxyacetate (MAc)	4.65	0.05-0.15	0.10-0.90	0.0055	0.0081	0.00028	0.0142		0.0013	0.238
fluoride ⁱ (F ⁻)	4.77 ^j	0.00125-0.0025	0.91	112	147	3.8	109	29.3		991
trifluoroethylamine (TFEA)	5.20	0.037-0.11	0.80		0.0057				0.0051	0.045
2,6-lutidine (LUT)	5.60	0.05-0.15	0.25-0.80	0.0019	0.0031					
phenylacetate (PhAc)	5.70	0.05-0.15	0.80		0.030					
acetate (Ac)	5.78 ^j	0.05-0.15	0.25-0.80	0.031	0.038	0.00117	0.034	0.0058	0.0108	0.85
hydroxylamine (NH ₂ OH)	5.90	0.20-0.41	0.20		0.32					
imidazole (IM)	6.31	0.05-0.15	0.20-0.50	0.020	0.026		0.050	0.0152	0.0176	0.39
N-methylmorpholine (NMM)	7.00	0.05-0.20	0.50	0.023				0.016		
cacodylate (CAC)	7.15	0.05-0.15	0.20-0.50	8.3	17.2	0.086	2.9	1.9		
2-methylimidazole (MIM)	7.23	0.05-0.15	0.25-0.75	0.039						
arsenate (ARS)	7.60	0.036-0.072	0.80		24.0		1.4			
Tris	7.87	0.02-0.20	0.25-0.75	0.05		0.0051				
ethanolamine (EA)	9.03	0.05-0.15	0.25-0.75				0.11			
n-butylamine (BA)	9.84	0.05-0.15	0.75				0.21			
hydroxide (OH ⁻)	16.93 ^k						1600			

^a Rates are calculated as k_N (eq 2). ^b In 45% dioxane-water (v/v), $\mu = 0.2$ (KCl), $T = 35^\circ \text{C}$. ^c Determined by half-neutralization. ^d Total buffer concentration. ^e Lower and upper limits of range studied are indicated. ^f Rate constants for **3a** are calculated as k_B ; however, they represent k_N terms (see Discussion). ^g The value of k_H obtained from multiple regression analysis of eq 1 is converted to water attack on the protonated amine by $k_{H_2O} = k_H K_a / 30.8$. ^h Calculated by dividing the dissociation constant of H_3O^+ by 30.8 M, the concentration of water in 45% dioxane-water (v/v). ⁱ Rate constants determined in the presence of 0.05 M acetate, pH 5.78. ^j Determined by potentiometric titration. ^k Calculated by dividing the dissociation constant for water, $3.63 \times 10^{-16} M^2$, by 30.8 M.

Table III. Experimental Conditions and Rate Constants^a for General Base Catalysis (k_B , $M^{-1} \text{ min}^{-1}$) of Phosphate Triester Hydrolysis^b

buffer	$pK_a^{B,c}$	concn ^d range, M	mole fraction ^e free base form	1a	1c	3a
2-methylimidazole (MIM)	7.23	0.05-0.15	0.25-0.75	0.033		
diethanolamine (DE)	8.61	0.05-0.15	0.25-0.75	0.205		
ethanolamine (EA)	9.03	0.05-0.15	0.20-0.80	0.86	30	0.194
n-butylamine (BA)	9.84	0.05-0.15	0.25-0.75	3.80		1.0
hydroxide ^f (OH ⁻)	16.93			61300	6.25×10^5	1200

^a Rates are reported as the free base from the buffer catalyzing the free base form of the phosphotriester. ^b Ionic strength maintained at 0.2 with KCl, $T = 35^\circ \text{C}$, 45% dioxane-water (v/v). ^c Determined by half-neutralization. ^d Total buffer concentrations. ^e Lower and upper limits of range studied are indicated. ^f The value of k_{OH} was determined from multiple regression analysis of eq 1.

replotted against the mole fraction buffer in the free base form (insert in Figures 2 and 3). At fraction free base = 0, the ordinate intercept value is k_{NH} , but $k_N = k_{NH}K_a/K_a^{B,24}$ at fraction free base = 1, the ordinate intercept value is k_B . Table III lists the second-order rate constants, k_B , for general base catalysis of $\sim OArX$ expulsion involving the free base forms of the triesters **1** and **3**. For triesters **2**, $k_B = 0$. In the case of **3a** only buffer catalysis expressed in terms of the rate constant, k_B , was found. For the triester functionalized with the quaternary ammonium group, **4a**, buffer catalysis can be described by the simple rate expression

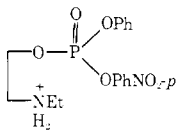
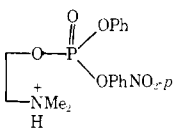
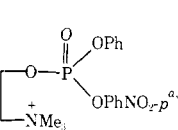
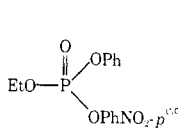
$$k^{PO} - k_O^{PO} = k_N[B]_T \left(\frac{K_a^B}{K_a^B + a_H} \right) \quad (5)$$

Values of k_N for **4a** are listed in Table II. The hydrolysis of ethyl *p*-nitrophenyl phenyl phosphate (**10**) to give *p*-nitrophenol also was catalyzed by the free base form of the buffer; values for k_N are given in Table IV.

Salt and Solvent Effects. The possibility that buffer catalysis (k_N or k_{NH}) was due to a specific salt effect was checked by using sodium perchlorate as the support electrolyte instead of potassium chloride. The hydrolysis of **2a** was carried out in 0.05-0.15 M acetate at pH 6.25 and $\mu = 0.2$ (NaClO₄) in 45% dioxane-water at 35°C . The results gave a value of $k_N = 0.038 M^{-1} \text{ min}^{-1}$, which is identical with that obtained when KCl was the electrolyte, indicating that catalysis is indeed due to the buffer and not a specific salt effect.^{25,26}

The effect of dioxane on the rate of attack by several

Table IV. Second-Order Rate Constants (k_N , $M^{-1} \text{ min}^{-1}$) for the Reactions of Buffers with Phosphotriesters

buffers				
H ₂ O	2.23×10^{-6}	2.19×10^{-6}	1.62×10^{-6}	
acetate	0.031	0.038	0.034	5.1×10^{-4}
fluoride	112	147	109 ^e	1.14 ^e
imidazole	0.020	0.026	0.050	
cianoacetate	0.0010	0.00138		
cacodylate	8.3	17.2	2.9	0.023
hydroxide			1600	4.51

^a In water ($\mu = 0.2$ (KCl)), the k_N values for acetate, fluoride, cacodylate, and hydroxide are 0.018, 29.3, 0.092, and 134 $M^{-1} \text{ min}^{-1}$, respectively. ^b The k_N value for *n*-butylamine is 0.21 $M^{-1} \text{ min}^{-1}$; for the reaction in water ($\mu = 0.2$ (KCl)) the value is 0.58 $M^{-1} \text{ min}^{-1}$. ^c In water ($\mu = 0.2$ (KCl)), the k_N values for acetate, fluoride, cacodylate, and hydroxide are 8.0×10^{-4} , 1.76, 0.041, and 6.51 $M^{-1} \text{ min}^{-1}$, respectively. ^d The k_N value for *n*-butylamine is 0.011 $M^{-1} \text{ min}^{-1}$; for the reaction in water ($\mu = 0.2$ (KCl)) the value is 0.053 $M^{-1} \text{ min}^{-1}$. ^e The k_N values in 85% dioxane–water for **4a** and **10** are 2200 and 2.41 $M^{-1} \text{ min}^{-1}$, respectively; the k_N for **4a** in 90% dioxane–water is $1.2 \times 10^4 M^{-1} \text{ min}^{-1}$.

Table V. ³¹P NMR Chemical Shifts (45% Dioxane–H₂O, 35 °C)

compd	chemical shift, ppm ^a	compd	chemical shift, ppm ^a
1a	−12.7 ^b	5 NHEt	−4.8 ^b
2a	−12.9	NMe ₂	−4.8 ^b
3a	−12.9	NHCH ₂ CF ₃	−4.9
4a	−13.5	NMe ₃ ⁺ , I [−]	−5.7
1b	−12.2 ^b	6 R ₁ = Et	+17.4
1c	−13.2 ^b	R ₁ = CH ₂ CF ₃	+16.5
7 X = <i>p</i> -NO ₂	−11.7	8 R ₁ = Et	+22.6
= <i>m</i> -NO ₂	−11.3	R ₁ = CH ₂ CF ₃	+20.6
= 2-Cl-4-NO ₂	−12.0		

^a Relative to external 85% H₃PO₄ (positive values are downfield).

^b Chemical shift moves about 0.5 ppm upfield as the amine becomes protonated.

nucleophiles on **4a** and **10** can be obtained from the data in Table IV. In the case of **10**, $k_N(45\% \text{ dioxane-water})/k_N(\text{water}) = 0.65, 0.64, 0.56, 0.21$, and 0.69 for fluoride, acetate, cacodylate, *n*-butylamine, and hydroxide ion, respectively; in the case of **4a** the same ratio = $3.7, 1.9, 31.5, 0.36$, and 11.9 for the identical nucleophilic series. Clearly the effect of mixed solvent is to decrease k_N in the absence of a neighboring positive charge but to increase k_N for anionic nucleophiles attacking **4a**. In the case of fluoride $k_N(90\% \text{ dioxane-water})/k_N(\text{water}) = 410$ for **4a**.

The effect of dioxane on k_B was studied by hydrolyzing **1a** in an aqueous media at 35 °C and $\mu = 0.2$ (KCl). Catalysis by both *n*-butylamine and ethanolamine was six times faster in water, whereas hydroxide was only 0.6 times as efficient.

Values for the rate coefficients k_{H_2O} and k_{OH} for **2a** and **4a** measured in 45% dioxane–D₂O (35 °C, $\mu = 0.2$, KCl) gave $k_{H_2O}/k_{D_2O} = 3.0$ and $k_{OH}/k_{OD} = 0.96$, respectively. For the C–O bond cleavage reaction of **2a**, $k_{H_2O}^{CO}/k_{D_2O}^{CO} = 1.15$. The deuterium solvent isotope effects on the k_N term associated with acetate catalysis are 1.4, 1.1, and 1.3 for **1a**, **2a** and **4a**, respectively; for imidazole catalysis they are 1.3, 2.6, and 1.4 for the series **1a–c**.

Products. The products arising from hydrolysis of the triesters were analyzed using proton decoupled ³¹P pulse Fourier transform NMR spectroscopy. The hydrolyses were carried out under identical conditions with those of the kinetic experiments at buffer concentrations of 0.5 M. Table V lists the chemical shifts of the various phosphate compounds that were detected. The hydrolysis of phosphotriesters **1** and **3a** in basic media (pH > 9) showed a rapid loss of their initial absorption

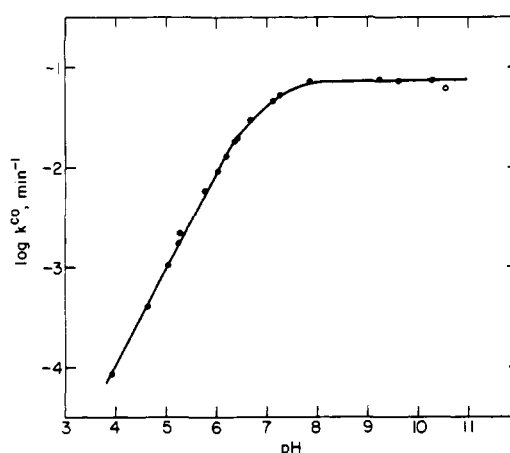


Figure 4. Dependence on pH of the observed pseudo-first-order rate constant for C–O bond cleavage for the hydrolysis of **2a** at 35 °C, 45% dioxane–water (v/v), $\mu = 0.2$ (KCl). The solid line is calculated from eq 3 and the rate constant in Table I. The rate of hydrolysis at pD 10.55 (○), 35 °C, 45% dioxane–D₂O (v/v), $\mu = 0.2$ (KCl), is also shown.

(~ -13 ppm) with a subsequent increase of a resonance at $\sim +17$ ppm indicating that the cyclic phosphoramidate **6** was formed. At longer times this resonance was replaced by one at lower field attributed to the cyclic phosphoramidate monoanion, **8**. Depending on pH some C–O cleavage occurred giving rise to a resonance at ~ -12 ppm which is attributed to **7**. Alkaline hydrolysis of triesters **2a** and **4a** gave rise only to resonances at -4.8 and -5.7 ppm corresponding to the acyclic phosphodiester **5** arising from loss of *p*-nitrophenol.

At neutral pH, the breakdown of all the phosphotriesters with the exception of **1c** and **4a** proceeds with formation of two resonances; one at ~ -5 ppm due to the acyclic phosphodiester **5** arising from loss of the respective phenol produced via P–O bond cleavage, and the other at ~ -12 ppm due to the aryl phenyl phosphodiester **7** produced via C–O bond cleavage. Hydrolysis of ester **4a** only gives rise to a singlet corresponding to the phosphodiester **5** due to the loss of *p*-nitrophenol. Hydrolysis of the triester **1c** with 2-chloro-4-nitrophenol as the leaving group, however, gives all three possible products, **5**, **6**, and **7**. Integration of each absorption peak gives the amount of each product formed under the respective conditions. No loss of phenol was detected under neutral or alkaline conditions.

A direct comparison of the P–O and C–O product distribution determined by ³¹P NMR and those calculated from

Table VI. Product Analysis of Phosphate Triester Reactions

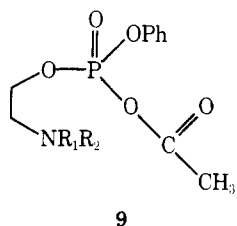
compd	buffer	P-O cleavage				C-O cleavage	
		acyclic		cyclic		³¹ P NMR ^a	calcd ^b
		³¹ P NMR ^a	calcd ^b	³¹ P NMR ^a	calcd ^b		
1a	imidazole ^c	75	71	0	0	25	29
1b	imidazole ^c	68	63	0	0	32	37
1c	imidazole ^c	59	71	33	23	8	6
1a	ethanolamine ^d	0	5	84	78	16	17
3a	ethanolamine ^d	9	0	75	96	16	4
1b	acetate ^e	70	68	0	0	30	32
1c	acetate ^e	100	99	0	0	0	1
3a	acetate ^e	18	21	0	0	82	79
1a	2-methylimidazole ^f	48	38	11	10	41	52

^a Values were determined by integration of the final spectrum. ^b Values were calculated as described in the text. ^c pH 6.55. ^d pH 9.25. ^e pH 5.90. ^f pH 7.46.

kinetic rate processes has been made in Table VI. The latter calculation was performed as follows: (1) the observed pseudo-first-order rate constants were initially divided into k^{PO} and k^{CO} on the basis of the fraction of -OArX produced; (2) k^{PO} was then partitioned into rate coefficients assigned to lyate and buffer catalysis (eq 1 and 2); (3) finally, the terms k_{OH} and k_{B} were associated with cyclic phosphoramidate formation, whereas k_{H} , $k_{\text{H}_2\text{O}}$, and k_{N} were associated with acyclic phosphodiester formation. However, in the case of **1c**, $k_{\text{H}_2\text{O}}$ must be assigned to cyclic phosphoramidate formation. Comparison of the distribution of products predicted from the kinetic rate expressions and those observed in the NMR experiments generally agrees within $\pm 5\%$.

No evidence for formation of acyl phosphates or phosphoramidates due to nucleophilic attack by carboxylates or amines at phosphorus was detected in the ³¹P NMR. However, when fluoride was the catalyst the appearance of a doublet with $J_{\text{PF}} = 933$ Hz indicated the formation of a phosphorus-fluorine bond. The doublets were centered at 6.6 ppm for **1**, 6.8 ppm for **2a**, 5.9 ppm for **3a**, and 7.2 ppm for **4a**. The other peak in the spectrum was a singlet due to the corresponding diester **5**. The nucleophilic attack by fluoride at phosphorus was confirmed with the use of ¹⁹F NMR. The initial spectrum contains a singlet at $\phi^* -122$ ppm due to NaF. Upon addition of the phosphate ester a doublet ($J_{\text{PF}} = 933$ Hz) centered at -76.7 ppm appears due to the formation of the phosphorus-fluorine bond. This doublet decays with time to give the singlet at $\phi^* -122$ ppm indicating that the phosphorofluoridate is hydrolyzed to the phosphate diester and fluoride ion. Therefore fluoride is acting in a catalytic mode.

Several experiments were designed to gain evidence for the formation of **9** in the presence of acetate. A ¹H NMR experi-



ment was conducted to test whether the acetyl phosphate **9** might be susceptible to an intramolecular transfer of the acetyl group to the amine, thereby forming a tertiary amide. The methylene protons adjacent to the amine group would be shifted approximately 0.6 ppm downfield if the amine became acetylated.²⁷ Hydrolysis of **1c** in acetate buffer gave a ¹H NMR spectrum with the chemical shift of the methylene protons adjacent to the amine (δ 2.75–3.25 ppm) remaining unchanged. Therefore the proposed acetyl phosphate intermediate apparently undergoes hydrolysis before any intramolecular acetyl transfer can occur. The difficulty in directly

observing the putative acyl phosphotriester is not unexpected;²⁸ the half-life for hydrolysis of acetyl dimethyl phosphate via C–O bond cleavage is estimated at 7.5 s at 34 °C, pH 6.0.²⁹ Trapping of **9** by hydroxylamine also proved unsuccessful.

A ³¹P NMR experiment was designed to investigate the origin of the oxygen in the phosphodiester **5** formed in the presence of acetate. Hydrolysis of **9** via C–O rather than P–O bond cleavage would lead to incorporation of an oxygen atom derived from acetate. The hydrolysis of both **1a** and **4a** in the presence of [¹⁸O]acetate–H₂¹⁶O produced **5** which exhibited only a single resonance at -5.25 ppm whereas the hydrolysis in acetate–H₂¹⁸O (67 atom % ¹⁸O) gave **5** whose ³¹P NMR (145 MHz) spectrum consisted of two singlets separated by 4.4 Hz corresponding to **5** containing both ¹⁶O and ¹⁸O. Consequently the decomposition of **9** appears to proceed via lyate species attack on phosphorus rather than carbon, presumably reflecting the ease of acetate displacement and catalysis by the neighboring ammonium group.

Discussion

The dependency of rate on pH for the P–O and C–O bond cleavage reactions of **1**, **2**, and **3** implicates participation by the amino group. A description of the pH–rate profiles for **1** and **2** requires the free base form of a group whose $\text{p}K_{\text{a}} \approx 7.8$ and 7.0, respectively. Values obtained from rapid potentiometric titration of **1** and **2** are 7.6 and 6.9, respectively. In addition the rate coefficients for the lyate species are greatly enhanced relative to appropriate phosphotriester reference compounds (vide infra). We will now consider the mechanism associated with the individual rate terms involving P–O bond cleavage.

Electrostatic Catalysis of Nucleophilic Attack. The k_{N} term in eq 2 which describes nucleophilic attack by buffer species on the conjugate acid forms of **1** and **2** is kinetically indistinguishable from external general acid catalysis of nucleophilic attack by the neighboring amino group (k_{NH}). The former description is preferred on the following grounds: (1) From the ³¹P NMR analysis (Table VI), no cyclic phosphoramidate **6** is formed in the presence of acetate during the hydrolysis of **1c** under conditions where **6** would be observable³⁰ and where $k_{\text{N}}/k_{\text{obsd}} = 0.96$. In the presence of imidazole **1a** and **1b** hydrolyze without formation of **6**³⁰ where $k_{\text{N}}/k_{\text{obsd}} \approx 0.58$ (**1a,b**). The observation of **6** during the hydrolysis of **1c** stems from the process associated with $k_{\text{H}_2\text{O}}$, not k_{N} . (2) The direct observation of P–F bond formation by ³¹P and ¹⁹F NMR in the reactions of **1**, **2a**, and **4a** defines a nucleophilic role for fluoride. (3) The small deuterium solvent isotope effect (<1.4) for the k_{N} term associated with acetate attack on **1a**, **2a**, and **4a** is in accord with a nucleophilic mechanism.¹⁶

In order to resolve the importance of proton transfer from the ammonium moiety to a phosphoryl oxygen during the course of reaction, the amino proton was replaced by a methyl group as in the choline ester, **4a**, so that the polar effect would

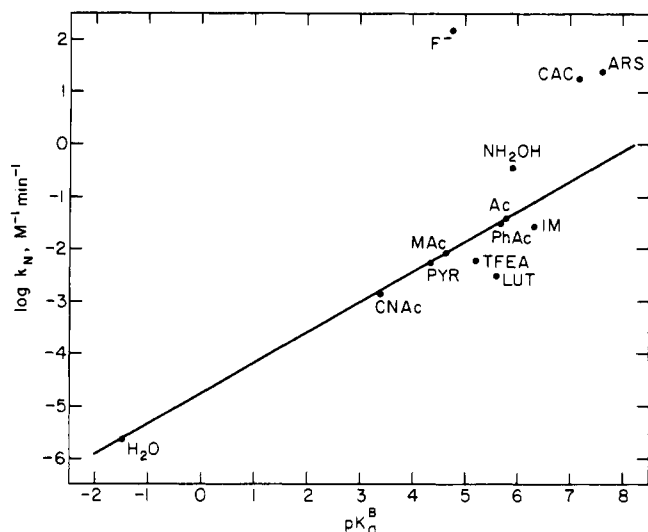


Figure 5. The dependence on basicity of the second-order rate constants (k_N) for the reactions of a series of buffers with the conjugate acid form of **2a** (Table II).

still be retained. The values of k_N for various buffer species are compared for **1a**, **2a**, and **4a** in Table IV. Most noteworthy is the near identity of the values of k_N across this series including such disparate nucleophiles as acetate, fluoride, imidazole, and cacodylate, providing further support for the proposed mechanism. In addition the rate constants ascribed to the attack of water on **4a** and to the equivalent process—nucleophilic attack by water on the protonated form of **1a**, **2a**, and **3a**—are in good agreement. Thus the juxtaposition of positive charge and not proton transfer is important for catalysis. It can be seen from Table IV that the rate enhancement in 45% dioxane–water arising from this polar effect relative to ethyl *p*-nitrophenyl phenyl phosphate, which possesses no intramolecular ammonium moiety, is ca. 350, 70, 125, and 100 for hydroxide, acetate, cacodylate, and fluoride, respectively, and 20 for *n*-butylamine.

Polar effects arising from a positively charged substituent in phosphate ester hydrolysis have been estimated at 25–50-fold for the attack of piperazine monocation on phosphoryl imidazole monocation,³¹ fivefold for the reaction of *o*-methylammonium phenolate with isopropyl methylphosphonofluoridate³² (an effect which drops off with distance, i.e., $o > m \sim p$), and 15-fold in the alkaline hydrolysis of the choline ester of methyl phosphonofluoridate relative to the ethyl ester.^{6a} Polar effects calculated for a through-bond induction model from the rates of alkaline hydrolysis of a series of α -substituted diethyl phosphonates²³ correlate with a $\rho_1 \approx 8$. Allowing for drop-off factors³⁴ of 2.0 per carbon and 2.0 per oxygen a $\rho_1 \approx 1$ can be calculated for the present series. With $\sigma \approx 0.9$ for Me_3N^+ ,³⁴ the rate of enhancement estimated for **4a** owing to such an inductive effect is only ca. eightfold, in agreement with an earlier estimate of fivefold estimated from the alkaline hydrolysis of choline acetate.³⁵ Thus the effects observed in this series are probably electrostatic in origin. This deduction is supported by the observation that the rate of nucleophilic attack by anions on **4a** is markedly accelerated by increasing dioxane content in the aqueous solvent, whereas that for **10** remains unchanged or slightly decreased. For attack by fluoride ion, the k_N ratio of **4a/10** in 85% dioxane–water is ca. 10^3 ; a linear correlation between $\log k_N$ and ϵ^{-1} is noted.³⁶ In the case of attack by a neutral amine the k_N ratio of **4a/10** is only ca. 20, suggesting that the increasing positive charge on the heteroatom in the transition state apparently attenuates the effect of the neighboring ammonium moiety. The sensitivity of the rate acceleration to the nature of the attacking nucleophile further suggests that stabilization of the

Table VII. Brønsted β Values

	β_{nuc}^a	β_{gb}^b	nucleophile	β_{1g}^c
1a	0.60	0.80	water ^d	0.82
2a	0.60		acetate	0.71
3a	0.40	0.88	fluoride	0.50
4a	0.56		cacodylate ^e	0.47
1b	0.65		cynoacetate ^d	0.92
2b	0.57		methoxyacetate ^d	0.95
1c	0.57		imidazole	0.75; ^d 0.09 ^e

^a Determined from plots of $\log k_N$ against pK_a^B (Figure 5). ^b Determined from plots of $\log k_B$ against pK_a^B (Figure 6). ^c Determined from plots of $\log k_N$ against pK_{a1g} for the series **1a–c**. ^d Determined from **1a** and **1c** only. ^e Determined from **1a** and **1b** only.

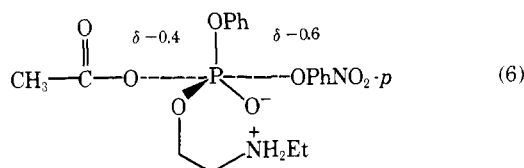
transition states rather than the ground state is important.³⁷ This phenomenon probably accounts, in part, for the successful synthetic employment of 2-(*N,N*-dialkylamino)-4-nitrophenyl phosphate as a phosphorylating agent toward alcohols³⁸ as well as the 1000-fold more rapid hydrolysis of 2-pyridinium phosphonic acid esters relative to the free base form.³⁹

A semiquantitative picture of the transition state(s) associated with the k_N term can be deduced from the respective Brønsted coefficients. The Brønsted coefficient will be viewed as a measure of the change in effective charge on the attacking or departing atom sensed by a substituent relative to that upon protonation.⁴⁰ Since in this system the nucleophiles and substituents on the leaving groups are separated by several atoms in the transition state(s), cross interactions arising from direct electrostatic effects ("Hine effect") will be minimized. Therefore the Brønsted coefficients may also be viewed as a rough measure of the amount of bond formation or bond cleavage in the transition state.⁴¹

A typical Brønsted plot is shown for nucleophilic attack (k_N) on the protonated form of **2a** in Figure 5. Values of β_{nuc} for the various triesters are listed in Table VII. Several salient features of this plot are worth noting: (1) attack by fluoride, cacodylate, and arsenate shows positive deviations of 10^4 , 10^2 , and 80-fold, respectively; (2) hydroxylamine is more reactive by only sixfold whereas 2,6-lutidine is less reactive by tenfold; (3) water shows the expected nucleophilic reactivity ($k_{\text{H}_2\text{O}}$, Table II). The high nucleophilicity of fluoride and arsenates toward tetrahedral phosphorus, the enhanced reactivity of hydroxylamine (α effect), and the decreased reactivity of the sterically hindered 2,6-lutidine are all in accord with a mechanism involving nucleophilic attack.⁴² Likewise Brønsted β_{1g} plots (Table VII) are linear (except for imidazole) and do not reveal a change in the nature of the rate-determining step about an addition intermediate.⁴⁰ However, it must be pointed out that the β_{1g} plots are based on a series partially comprised of meta and ortho substituents so that accuracy is not better than $\pm 20\%$. The reaction of imidazole apparently involves a change in mechanism from nucleophilic to general-base-catalyzed solvent attack because the deuterium solvent isotope effect changes from $k_{\text{H}_2\text{O}}/k_{\text{D}_2\text{O}} \approx 1.3$ for 2-chloro-4-nitro- and *p*-nitrophenolate leaving groups to 2.6 for the *m*-nitrophenolate—a phenomenon previously encountered in imidazole catalysis of acyl ester hydrolysis with progressively poorer leaving groups.⁴³ To our knowledge there have been no reports of biphasic Brønsted plots (β_{nuc} or β_{1g}) in nucleophilic displacements at phosphorus owing to changes in a rate-determining step.

The data given above permits us to make a tentative assignment of the "effective charge" distribution for the reactions of fluoride and oxygen nucleophiles with the phosphotriesters but does not require us to include or exclude pentacovalent species associated with these transition states. Since the changes in charge on a given group in going from reactant to transition state to products are equal to the change for the overall equilibrium (i.e., $\beta_{\text{eq}} = \beta_{\text{r}} - \beta_{\text{p}}$ where β_{eq} relates to the

effect of substituents on the equilibrium constant and β_f and β_r on the forward and reverse rate constants) it is useful to have the charge distribution in the reactant and product ground state as a starting point for applying β_f and/or β_r . A value of $\beta_{eq} = 1.2$ has been estimated for the complete transfer of $[\text{PO}_3^{2-}]$ between various amine nucleophiles and a series of substituted pyridinium phosphoramidates.⁴⁴ The equilibrium transfer of $[(\text{RO})_2\text{PO}]$ between oxy anions and amines has not been measured; however, a $\beta_{eq} \approx 1.1$ can be estimated from rate data for the attack of oxy anions on substituted 2-(aryloxy)-2-oxo-1,3,2-dioxaphosphorinans owing to the symmetry of the displacement reaction.⁴⁵ For the attack by acetate on **1a** the following approximate distribution of charges in the transition state applies (6). As is characteristic of coupled transition states



for a displacement process β_{nuc} increases where β_{lg} decreases, Table VII (Hammett behavior), a trend more clearly observed in the oxy anion–dioxaphosphorinan system owing to a greater range in ΔpK_a . The rate acceleration of **4a** relative to **10** (70–350 fold—of which ca. 1.0 kcal/mol is due to inductive effects and 1.6–2.6 kcal/mol is due to electrostatic interactions) suggests that the positive charge in the transition state is in close proximity (ca. 3.5–5.6 Å) to the phosphoryl moiety.⁴⁶

Values of β_{nuc} for reactions of oxy anions with several other phosphate triesters are 0.48 for 2-(4-nitrophenoxy)-2-oxo-1,3,2-dioxaphosphorinan,⁴⁵ 0.52 for 2,4-dinitrophenyl dibenzyl phosphate,⁴⁷ 0.59 for isopropyl methylphosphonofluoridate,³³ and 0.42 for diisopropyl phosphorofluoridate,⁴⁸ similar to the present case (Table VII). Thus the electrostatic catalysis exhibited by the ammonium function acts to lower the activation energy without substantially shifting the transition state on the reaction coordinate.

From the observed kinetics, it is apparent that the free base form of the trifluoroethylamino moiety is capable of accelerating nucleophilic attack by buffer species, e.g., the rate of acetate attack is ca. 50-fold greater than in the phosphotriester but 30-fold less than the quaternary ammonium species. The value of $\beta_{nuc} \approx 0.4$ is somewhat lower than that obtained for the fully positively charged ammonium groups (Table VII); however, similar deviations for fluoride and cacodylate are seen in the Brønsted plot (Figure 6), indicative of nucleophilic catalysis. In the absence of a structure–reactivity correlation for this displacement process, one cannot empirically predict the magnitude of the rate effect caused by this substitution.⁴⁹ It is possible that hydrogen bonding to the phosphoryl oxygen is important in this case owing to the increased acidity of the N–H moiety caused by the CF_3CH_2 substituent. At lower pH, where this group is present as its conjugate acid, the rate coefficient for hydrolysis agrees with that for **1a**, **2a**, and **4a** (Table II), consistent with the postulated nucleophilic displacement process.

Spontaneous Hydrolysis. The $k_{\text{H}_2\text{O}}$ term defined in eq 1 is associated with two different mechanisms depending on the identity of the phenolate leaving group. For **1c** (2-chloro-4-nitrophenolate), observation of the cyclic phosphoramidate implicates intramolecular nucleophilic attack. With *p*-nitrophenolate as the leaving group, the measurement of a deuterium solvent isotope effect ($k_{\text{H}_2\text{O}}/k_{\text{D}_2\text{O}} \approx 3$) for **2a** and the absence of cyclic phosphoramidate formation of **1a** implicates an intramolecular general base role for the amino moiety. A similar mechanism apparently pertains to **1b** which hydrolyzes with loss of *m*-nitrophenolate, since *p*-nitrophenolate and

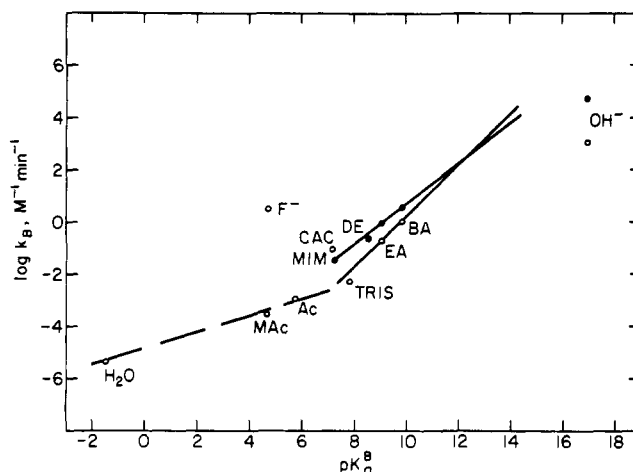


Figure 6. The dependence on basicity of the second-order rate constants (k_B) for the reaction of a series of buffers with the conjugate base form of **1a** (●, Table III) and with the conjugate base form of **3a** (○, Tables II and III). The dashed line is drawn through buffers acting as nucleophilic catalysts.

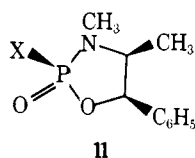
m-nitrophenolate show a decreased sensitivity ($\beta_{lg} = 0.2$) to the identity of the leaving group supporting a change in mechanism relative to **1c** ($\beta_{lg} > 0.8$). Moreover, $k_{\text{H}_2\text{O}}$ for **1a** and **3a** responds to the pK_a of the amino moiety decreasing 100-fold upon replacing Et with CF_3CH_2 —where $\Delta pK_a \approx 5$. Thus the kinetically indistinguishable process, i.e., attack by hydroxide on the protonated triester (k'_{OH}), which should be nearly invariant despite changes in amine pK_a , can be ruled out by the inequivalence between the rate coefficients calculated for this process across the series **1a**, **2a**, **3a**, and **4a**.⁵⁰ The above deuterium solvent isotope effect ($k'_{\text{OH}}/k'_{\text{OD}} = 1.7$) is not in accord with an inverse effect predicted for a specific-base-catalyzed reaction.¹⁶ The efficiency of either the nucleophilic or general base intramolecular processes is approximately 200-fold over the respective electrostatic assisted water attack.

General Base Catalysis of Intramolecular Nucleophilic Attack. The k_B term in eq 2 and the k_{OH} term in eq 1 are associated with a mechanism in which buffer and lyate species act as general base catalysts for intramolecular amine attack. This conclusion is based on the following facts: (1) the rapid formation of the cyclic phosphoramidate **6** during the hydrolysis of **1** or **3** in basic media is apparent from the ^{31}P NMR data (Table V) as well as from the observation that the rates of phenoxide expulsion from **1a–c** and **6** ($R_1 = \text{Et}$) are identical—consistent with rate-determining breakdown of **6** in their overall hydrolysis; (2) replacement of the amino proton by a methyl group results in a disappearance of the k_{OH} and k_B terms suggesting that a proton abstraction process is associated with the above kinetic terms.

Two related questions arise: does the cyclization process proceed through a pentacovalent intermediate and what is the mechanism of general base catalysis? Evidence pertaining to the lifetime of the pentacovalent intermediate can be summarized as follows.

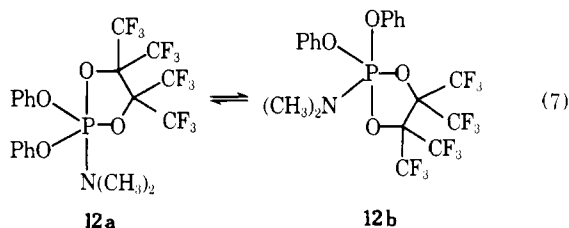
(1) Although ample precedent exists for pentacovalent species containing a five-membered ring spanning apical and equatorial positions,⁵¹ the stabilities of such intermediates vary widely depending on the nature of the substituting ligands.⁵² An appropriate criterion for a pentacovalent intermediate often may be obtained from the stereochemical course of the substitution reaction.⁵³ Employing the widely accepted hypothesis that initial attack and departure occur from only apical positions, the demonstration in a given substitution reaction that the process proceeds with retention of configuration requires

at least one pseudorotation event involving a pentacovalent species. Reactions of 1,3,2-oxazaphospholidines proceed with inversion of configuration at phosphorus for endocyclic P-N cleavage but retention of configuration at phosphorus for displacement of labile exocyclic 2 substituents.⁵⁴ It can readily be demonstrated that the stereochemical course of exocyclic substitution in **11** requires a pseudorotation event regardless



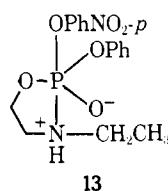
of whether nucleophilic attack occurs opposite -N- or -O-, the latter course being preferred owing to the greater apicophilicity of oxygen. Consequently, the observed stereochemical course for endocyclic P-N and exocyclic P-O bond cleavage may not proceed through a common intermediate, prompting the suggestion that the endocyclic process is a simple S_N2 displacement.

(2) Although the pseudorotation involving trigonal bipyramidal structures **12a** and **12b** has been observed by low-temperature ^{19}F NMR owing to the observed difference in apicophilicity between amino and phenoxy groups of 7-8



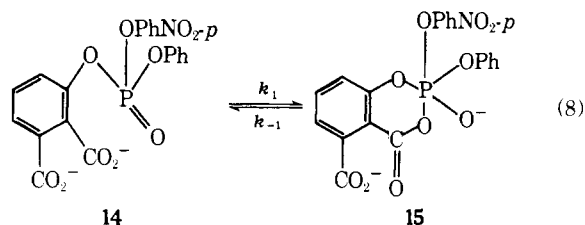
kcal/mol,⁵⁵ pseudorotations involving the protonated amino species have not been observed on the NMR time scale owing to the diminished barrier for pseudorotations caused by the electronegative group $(\text{R})_2\text{NH}^+$. Hence there is no direct physical evidence for the existence of a pentacovalent species analogous to that required in the above displacement reaction.

(3) An estimate of the pK_a of the putative intermediate **13** from the Branch-Calvin equation gives a value of 5.3; this is probably a maximal pK_a owing to back-bonding ($\text{p}_\pi\text{-d}_\pi$) in the P-N bond stabilizing the conjugate base species.⁵⁶ Consequently the proton transfer from **13** to the base catalysis em-



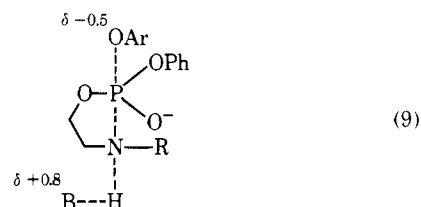
ployed here is thermodynamically favorable. However, the observed β for general base catalysis in **1a** is 0.8 (Figure 6), not the $\beta = 0$ expected for a thermodynamically favored stepwise proton transfer process from **13** through either a diffusion-limited (trapping of the intermediate by proton removal) or a preassociation mechanism featuring catalysis of the addition step through hydrogen bonding.⁵⁷ The observed β value, however, can be accommodated by rate-determining decomposition of **13** stabilized by hydrogen bonding of the conjugate acid species of the buffer to the amino group provided that the rate of decomposition of **13** exceeds that of diffusion away of the catalyst which is ca. 10^{11} s^{-1} . Thus the failure to observe Eigen-type behavior suggests that **13**, if it exists, has a lifetime of $<10^{-11} \text{ s}$.

(4) The rate of decomposition, k_{-1} , of the pentacovalent species **15** which is a required intermediate in the decomposi-



tion of **14** owing to the observation of competing exo- and endocyclic cleavage has been estimated from structure-reactivity correlations as ca. $3.5 \times 10^{10} \text{ s}^{-1}$.^{2b} From structure-reactivity correlations the rates of decomposition of monoester monoanions through their zwitterionic intermediates RXHPO_3^{2-} are ca. 10^2 greater for an amine vs. a phenol leaving group, where the conjugate acid of the amine and the phenol have an identical $\text{pK}_a \approx 3.5$.^{1d} For expulsion of a phenolate vs. phenol, i.e., decomposition of the monoester dianion vs. the monoanion, the ratio is ca. 10 for a phenol of $\text{pK}_a \approx 3.5$. Although the driving force obviously is greater in the latter examples, the greater ease of P-N vs. P-O cleavage should be retained, so that a minimal k_{-1} for **13** should be ca. 10^{12} s^{-1} . Consequently the observed general base catalysis is not an example of unenforced catalysis by hydrogen bonding,⁵⁸ since the intermediate should not be in equilibrium with the bulk solution with respect to proton transfer.⁵⁹ The maximal value of k_{-1} approaches that expected for a vibrational frequency suggesting that **13** may not have a finite lifetime.

In view of the above considerations, a concerted mechanism coupling amine attack and proton transfer is postulated for the observed general base catalysis (eq 9) with little development of the charge on the departing phenoxide.



Evidence supporting this mechanism can be summarized as follows:

(1) The amino site undergoes a large change in pK_a upon addition to phosphorus that converts an unfavorable to a favorable proton transfer with respect to the catalyst, permitting but not requiring a concerted pathway (libido rule).⁶⁰

(2) The Brønsted β_{gb} values for general base catalysis for attack by EtNH^- and $\text{CF}_3\text{CH}_2\text{NH}^-$ are 0.8 and 0.9, respectively. This change is in the opposite direction from what one might initially expect from the considerations of Leffler and Hammond,⁶¹ which predict that the proton transfer should occur with an earlier transition state for the less basic amine (recall that the proton transfer from **13** is thermodynamically favorable). However, the observed behavior is consistent with linking the proton transfer and P-N bond development and may be described as a substituent effect perpendicular to the reaction coordinate.⁶²

(3) The β_{1g} for the term k_{OH} of **1a-c** is ca. 0.6 and includes an effect by the phenol on the sensitivity of phosphorus to nucleophilic attack as well as the stabilization of the leaving group. For intramolecular attack by carboxylate on triester phosphorus, $\beta_{1g} \approx -1.4$ of which ca. -0.30 may be attributed to polar effects on phosphorus. Whereas in the carboxylate case β_{1g} approximates β_{1g} for equilibrium transfer, the present value suggests much less effective charge on the oxy anion and to a rough approximation less bond cleavage.

The unusual feature of the above mechanism that emerges is the early transition state with respect to the leaving group but the late transition state with respect to proton transfer.

Since catalysis does not arise from proton trapping of a pentacovalent species, it apparently represents transition-state stabilization arising from hydrogen-bond or concerted catalysis. Since proton abstraction from the amino nitrogen is not thermodynamically feasible in the absence of P–N bond development, catalysis of amine attack represents a concerted reaction mechanism, in the sense that it does not proceed stepwise. Alternatively catalysis may represent hydrogen-bonding stabilization of the rate-determining decomposition of **13** following proton transfer provided that this rate exceeds that of diffusional separation of **13** and the conjugate acid catalyst. The value of β is within the range of values that have been observed for stable hydrogen bonds, with no intervening water molecule, that live in a broad, single potential well.⁶³ If there is little or no barrier for proton transfer and for addition of the amino group within the catalyst–substrate complex then the effective charge distribution transition state should resemble (9). Although a choice between these two postulates is presently not possible, both limit the lifetime of the putative **13** to $<10^{-12}$ s.

Conclusions

The present triester system exhibits a variety of competing reaction pathways including electrostatic assisted nucleophilic displacement, intramolecular general base catalysis of water attack, and general-base-catalyzed intramolecular nucleophilic displacement emphasizing the similarity in the free energy of activation for the various processes. Structure–reactivity correlations lead to the construction of transition states for the two nucleophilic displacement processes that are in accord with coupled or concerted bond formation and cleavage. Even in the case where a cyclic product is found, no evidence has been obtained for an intervening pentacovalent species whose lifetime exceeds 10^{-12} s. Thus displacement reactions by nitrogen nucleophiles on phosphorus in aqueous media may only occur via an in-line mechanism so that the stereochemical course is restricted to one of inversion.

Acknowledgment. The authors wish to thank Dr. K. DeBruin and Dr. W. P. Jencks for their constructive comments. Support of this research by Public Health Service Grant GM13306 is also gratefully acknowledged.

References and Notes

- For a review of phosphate ester hydrolyses, see (a) T. C. Bruice and S. J. Benkovic, "Bioorganic Mechanisms", Vol. II, W. A. Benjamin, New York, 1966, Chapter 5; (b) S. J. Benkovic in "Comprehensive Chemical Kinetics", Vol. 10, C. H. Bamford and C. F. H. Tipper, Eds., American Elsevier, New York, 1971, p. 1; (c) S. J. Benkovic and K. J. Schray in "Transition States of Biochemical Processes", R. D. Gandour and R. L. Schowen, Eds., Plenum Press, New York, 1978, p. 493; (d) S. J. Benkovic and K. J. Schray in "The Enzymes", Vol. VIII, 3rd ed., P. D. Boyer, Ed., Academic Press, New York, 1973, p. 201.
- (a) R. H. Bromilow, S. A. Khan, and A. J. Kirby, *J. Chem. Soc. B*, 1091 (1971); (b) R. H. Bromilow, S. A. Khan, and A. J. Kirby, *J. Chem. Soc., Perkin Trans. 2*, 911 (1972); (c) G. M. Blackburn and M. J. Brown, *J. Am. Chem. Soc.*, **91**, 525 (1969); (d) S. S. Simons, *ibid.*, **96**, 6492 (1974).
- D. A. Usher, D. I. Richardson, Jr., and D. G. Oakenfull, *J. Am. Chem. Soc.*, **92**, 4699 (1970).
- (a) R. Kluger and J. L. W. Chan, *J. Am. Chem. Soc.*, **98**, 4913 (1976); (b) R. A. Naylor and A. Williams, *J. Chem. Soc., Perkin Trans. 2*, 1908 (1976).
- (a) G. J. Durant, J. H. Turnbull, and W. Wilson, *Chem. Ind. (London)*, 157 (1958); (b) D. M. Brown and G. O. Osborne, *J. Chem. Soc.*, 2590 (1957); (c) J. S. Loran and A. Williams, *J. Chem. Soc., Perkin Trans. 2*, 64 (1977); (d) P. A. Manninen, *Acta Chem. Scand., Ser. B*, **32**, 269 (1978); (e) R. A. Lazarus and S. J. Benkovic, unpublished results.
- (a) L. Larsson, *Acta Chem. Scand.*, **11**, 1131 (1957); (b) L. E. Tammelin, *ibid.*, **11**, 859 (1957).
- L. F. Fieser, "Experiments in Organic Chemistry", 3rd ed., D. C. Heath, Boston, Mass., 1957, p. 284.
- I. Dilaris and G. Eliopoulos, *J. Org. Chem.*, **30**, 686 (1965).
- M. H. Litt, A. J. Levy, and T. G. Bassiri, *Chem. Abstr.*, **65**, 7065 (1966).
- C. Brown, J. A. Boudreau, B. Hewitson, and R. F. Hudson, *J. Chem. Soc., Perkin Trans. 2*, 888 (1976).
- M. Cohn and A. Hu, *Proc. Natl. Acad. Sci. U.S.A.*, **75**, 200 (1978).
- A. Albert and E. P. Seargent, "The Determination of Ionization Constants", Chapman and Hall, London, 1971.
- H. M. N. H. Irving and U.S. Mahnot, *J. Inorg. Nucl. Chem.*, **30**, 1215 (1968).
- H. S. Harned and L. D. Fallon, *J. Am. Chem. Soc.*, **61**, 2374 (1939).
- T. H. Fife and T. C. Bruice, *J. Phys. Chem.*, **65**, 1079 (1961).
- P. M. Laughton and R. E. Robertson, "Solute-Solvent Interactions", J. F. Coetzee and C. D. Ritchie, Eds., Marcel Dekker, New York, 1969, Chapter 7.
- W. P. Jencks, "Catalysis in Chemistry and Enzymology", McGraw-Hill, New York, 1969, p. 569.
- A. J. Kirby and M. Younas, *J. Chem. Soc. B*, 510 (1970).
- T. C. Bruice and J. J. Bruno, *J. Am. Chem. Soc.*, **83**, 3494 (1961).
- Chem. Eng. News*, **55**(31), 14 (1977).
- $\phi^* = {}^{19}\text{F}$ shift of sample relative to CFCl_3 , $\phi_R^* = {}^{19}\text{F}$ shift of reference relative to CFCl_3 , and $\delta_S = {}^{19}\text{F}$ shift of sample relative to ${}^{19}\text{F}$ shift of reference. The reference used was $\text{CF}_3\text{COOH}/\text{D}_2\text{O}$, which has $\phi_R^* 76.55$ ppm.
- L. Zervas and C. Hamalidis, *J. Am. Chem. Soc.*, **87**, 99 (1965).
- P. R. Bevington, "Data Reduction and Error Analysis for the Physical Sciences", McGraw-Hill, New York, 1969.
- The term $k_N[\text{B}]_T \left(\frac{K_a^B}{K_a^B + a_H} \right) \left(\frac{a_H}{K_a + a_H} \right)$ is kinetically equivalent to the term $k_{NH}[\text{B}]_T \left(\frac{a_H}{K_a^B + a_H} \right) \left(\frac{K_a}{K_a + a_H} \right)$ where k_{NH} measures general acid buffer catalysis of intramolecular amine attack on phosphorus.
- P. Salomaa, A. Kankaanperä, and M. Lahti, *J. Am. Chem. Soc.*, **93**, 2084 (1971).
- Specific salt effects have been seen before in the hydrolysis of 2,4-dinitrophenyl dibenzyl phosphate; however, these were at much higher salt ($\mu = 1.0$) and buffer (1 M) concentrations. D. Gorenstein and Y. G. Lee, *J. Am. Chem. Soc.*, **99**, 2258 (1977).
- For example, the methylene protons adjacent to the nitrogen in morpholine appear at 2.87 ppm, whereas in *N*-acetylmorpholine their chemical shift is at 3.45 ppm.
- The problem of identifying an acyl phosphotriester has been encountered before.²⁶
- R. Kluger and P. Wasserstein, *Biochemistry*, **11**, 1544 (1972).
- The rate of P–N bond cleavage of **6** ($R_1 = \text{Et}$) is faster than the rate of P–O bond cleavage of **1a–c** below pH 6.2, 6.4, and 5.4, respectively, so that **6** will only be observable at higher pH values.
- G. J. Lloyd, C. M. Hsu, and B. S. Cooperman, *J. Am. Chem. Soc.*, **93**, 4889 (1971).
- J. Epstein, R. E. Plapinger, H. O. Michel, J. R. Cable, R. A. Stephani, R. J. Hester, C. Billington, Jr., and G. R. List, *J. Am. Chem. Soc.*, **86**, 3075 (1964).
- G. Aksnes and J. Songstad, *Acta Chem. Scand.*, **19**, 893 (1965).
- J. Hine, "Structural Effects on Equilibrium in Organic Chemistry", Wiley-Interscience, New York, 1975, Chapter 3.
- B. Hansen, *Acta Chem. Scand.*, **16**, 1927 (1962).
- A plot of $\log k_F$ vs. $1/\epsilon$ gives a slope of 12.88 and an intercept of 1.64. For a discussion of dielectric effects on rates see E. S. Amis, "Solvent Effects on Reaction Rates and Mechanism", Academic Press, New York, 1966.
- B. Holmquist and T. C. Bruice, *J. Am. Chem. Soc.*, **91**, 2985 (1969).
- Y. Taguchi and Y. Mushika, *J. Org. Chem.*, **40**, 2310 (1975).
- J. S. Loran, R. A. Naylor, and A. Williams, *J. Chem. Soc., Perkin Trans. 2*, 418 (1977).
- M. J. Gresser and W. P. Jencks, *J. Am. Chem. Soc.*, **99**, 6963 (1977).
- D. A. Jencks and W. P. Jencks, *J. Am. Chem. Soc.*, **99**, 7948 (1977).
- (a) Both fluoride and arsenates react to give complete P–O bond cleavage. (b) H. J. Brass and M. L. Bender, *J. Am. Chem. Soc.*, **94**, 7421 (1972).
- J. F. Kirsch and W. P. Jencks, *J. Am. Chem. Soc.*, **86**, 837 (1964).
- (a) S. J. Benkovic and E. J. Sampson, *J. Am. Chem. Soc.*, **93**, 4009 (1971); (b) W. P. Jencks and M. Gilchrist, *ibid.*, **86**, 1410 (1964); (c) G. W. Jameson and J. M. Lawlor, *J. Chem. Soc. B*, 53 (1970).
- The derived value of β_{eq} assumes that the nucleophilic displacement does not involve an intermediate: S. A. Khan and A. J. Kirby, *J. Chem. Soc. B*, 1172 (1970).
- Estimated from simple electrostatic theory assuming point charges and $\epsilon = 36.3$. Nucleophilic attack by acetate is accelerated in less polar solvents in accord with a decrease in the medium dielectric. This is apparently much more important than any effects due to interaction of acetate and the phosphotriester.²⁶
- Taken from the line drawn through water and acetate as nucleophiles.²⁶
- M. Kilpatrick and M. L. Kilpatrick, *J. Phys. Chem.*, **53**, 1371 (1949).
- An estimate based on various electrostatic models is subject to too many uncertainties. See C. L. Liotta, W. F. Fisher, G. H. Greene, Jr., and B. L. Joyner, *J. Am. Chem. Soc.*, **94**, 4891 (1972).
- $k'_{OH} = k_{H_2O}K_a/K_w = 1.0 \times 10^6, 7.8 \times 10^6, 1.2 \times 10^9$, and $1.6 \times 10^3 \text{ M}^{-1} \text{ min}^{-1}$ for **1a**, **2a**, **3a**, and **4a**, respectively.
- F. H. Westheimer, *Acc. Chem. Res.*, **1**, 70 (1968).
- S. Trippett, *Phosphorus Sulfur*, **1**, 89 (1976).
- R. Luckenbach, "Dynamic Stereochemistry of Pentacoordinated Phosphorus and Related Elements", Georg Thieme Verlag, Stuttgart, 1973.
- D. B. Cooper, C. R. Hall, J. M. Harrison, and T. D. Inch, *J. Chem. Soc., Perkin Trans. 1*, 1969 (1977).
- S. Trippett and P. J. Whittle, *J. Chem. Soc., Perkin Trans. 1*, 2302 (1973).
- G. E. Branch and M. Calvin, "The Theory of Organic Chemistry", Prentice-Hall, Englewood Cliffs, N.J., 1941, p. 204. The pK_a of **13** was calculated based on an initial value of 7.64 for **1** and both charge and substituent effects upon cyclization to **13**.
- W. P. Jencks, *Acc. Chem. Res.*, **9**, 425 (1976).
- P. R. Young and W. P. Jencks, *J. Am. Chem. Soc.*, **99**, 1206 (1977).

- (59) Abstraction of a proton from **13** by water can be estimated at 10^{-1} s^{-1} from $10^{10} K_w/K_a$.
 (60) W. P. Jencks, *J. Am. Chem. Soc.*, **94**, 4731 (1972).
 (61) (a) J. E. Leffler, *Science*, **117**, 340 (1953); (b) G. S. Hammond, *J. Am. Chem.*

- Soc.*, **77**, 334 (1955).
 (62) W. P. Jencks, *Chem. Rev.*, **72**, 705 (1972).
 (63) M. M. Kreevoy, T. Liang, and K. Change, *J. Am. Chem. Soc.*, **99**, 5207 (1977).

ESR of Transient Radicals during Pyrolysis of Fluids

Ralph Livingston,* Henry Zeldes, and Mark S. Conradi

Contribution from the Chemistry Division, Oak Ridge National Laboratory, Oak Ridge, Tennessee 37830. Received February 1, 1979

Abstract: ESR equipment has been developed for directly observing labile free radicals that are present at high temperatures. A pressurized fluid is heated as it slowly flows through the microwave cavity of the spectrometer. Temperatures to 566 °C and pressures to 140 kg/cm² have been used. Radicals are identified from well-resolved hyperfine structure. Spectra of cyanoisopropyl from the decomposition of azobisisobutyronitrile in solution at 155–185 °C and hydroxyisopropyl from 2% di-*tert*-butyl peroxide in isopropyl alcohol at 173–258 °C are reported. Indenyl is reported from indene in benzene at 533 °C and in tetralin at 471 °C. 1,2-Diphenylethyl has been observed from solutions of 1,2-diphenylethane in benzene from 460 to 560 °C. For dilute solutions of 1,2-diphenylethane in toluene the benzyl radical is obtained, while for more concentrated solutions a mixture of radicals is present in the following equilibrium for which $K = 10 \pm 3$ at 560 °C and 105 kg/cm²: $\text{C}_6\text{H}_5\text{CH}_2\text{CH}_2\text{C}_6\text{H}_5 + \text{C}_6\text{H}_5\text{CH}_2 \rightleftharpoons \text{C}_6\text{H}_5\text{CHCH}_2\text{C}_6\text{H}_5 + \text{C}_6\text{H}_5\text{CH}_3$. Diphenylmethyl is obtained from the dissociation of tetraphenylethane as a dilute solution in benzene and in 50:50 benzene–diphenylmethane. ESR parameters are given in the latter solvent at 420 °C. The formation of diphenylmethyl from diphenylmethane as a consequence of impurities has been examined, and diphenylmethane that has been initially air oxidized will form diphenylmethyl upon heating. Cumyl is obtained from cumene at 560 °C. α -Methylstyrene is a final product but not dicumyl. Dicumyl in benzene solution at 560 °C decomposes to give disproportionation products cumene and α -methylstyrene. The addition of α -methylstyrene or 1,2-diphenylethane to cumene at 560 °C markedly enhances the production of cumyl. Cumyl is seen from air-saturated cumene at 350 °C. *p*-Cumyl from *p*-cymene, phenylethyl from ethylbenzene containing styrene, and *o*-xyl from *o*-xylene containing 1,2-diphenylethane have been observed at 560 °C. Hyperfine couplings and *g* values are given and compared with room temperature values, and a discussion involving kinetic parameters is presented.

We have started an electron spin resonance program for the study of free radicals formed in fluids during the course of pyrolysis. Our aim is to obtain a better understanding of the role played by free radicals in high-temperature processes by directly observing these reactive intermediates at steady-state concentration. In this paper, we first describe newly developed techniques and then concentrate largely on the pyrolysis of aromatic hydrocarbons that give rise to benzylic radicals. The substances are of general interest as model compounds in coal-conversion processes and in the combustion of aromatic fuels.

A liquid sample, either the neat compound or a solution, is pressurized and then heated as it slowly flows through the microwave cavity of an ESR spectrometer. The temperature needed to sustain a large enough radical concentration is usually greatly above the critical temperature of the substance used. The reason for pressurizing the system is to maintain a high fluid density. In addition to providing an adequate amount of sample in the microwave cavity, the high density quenches the angular momentum of overall rotation of the radicals. This reduces the ESR line width contribution from the spin-rotational mechanism as described by Schaafsma and Kivelson,¹ who concluded that the contribution varies inversely as the pressure and directly with $T^{3/2}$. A significant finding of this work is that lines at the high pressure are sharp enough to give well-resolved spectra.

Singer and Lewis^{2,3} have studied resolved ESR hyperfine structure after pyrolysis of several aromatic hydrocarbons in a silica tube located in the microwave cavity of a spectrometer. Either the neat hydrocarbon or more often a solution in *m*-quinquephenyl (bp 540 °C) was used. The authors point out that "the free radicals must be sufficiently stable so that a reasonably intense EPR signal can be observed. Adequate

stable radical concentrations can usually be achieved by thermally quenching the carbonization reactions." In the present work, the spectra of transient radicals were observed with a slowly flowing sample at the pyrolytic temperature. In some cases, the burn-up rate of the sample was so high that a static sample could not have been used. In general, the radicals reported are highly labile, and increased signal strength could usually be achieved by increasing the temperature.

Experimental Section

Essential features of the flow system are shown in Figure 1. The sample was contained in a glass reservoir of 100-mL capacity, and the purging gas, used to remove dissolved oxygen, was helium unless otherwise stated. The high-pressure pump was of the type used for high-pressure liquid chromatography (Waters Model 6000 A) and was normally operated at 1.0 mL/min. Apart from the silica capillary that served as the pyrolysis cell, the tubing of the high-pressure system was 1.59 mm o.d. stainless steel. The silica capillary was 1.4 mm i.d. and 4.7 mm o.d. It connected to the high-pressure stainless steel tubing through seals containing Teflon packing.⁴ The rectangular microwave cavity operated in the TE₁₀₂ mode (Varian Model V-4531) and could accommodate objects up to 11 mm in diameter. Pressure transducers were included before and after the pyrolysis cell, and these indicated on chart recorders provided with a scale range of 0–211 kg/cm² (0–3000 psi). The cell and seals were statically tested at 280 kg/cm², and safety trips for turning the equipment off were set at 211 kg/cm². The transducers were calibrated with a precision Bourdon gage supplied by Heise. The throttling valve (Hoke Model 1666 G1Y) was set manually and adjusted as needed during an experiment in order to maintain the desired pressure. The setting of this valve was occasionally troublesome because the flow coefficient (C_v value of 0.0008 fully opened) was larger than ideal. We eventually hope to automate this portion of the equipment. Small-diameter Teflon tubing was used to return liquid from the throttling valve to the reservoir at atmospheric pressure, and, if sufficient gas formed during pyrolysis, it was